Anthropogenic nitrogen deposition decouples relationships with decomposing microbes, altering SOM molecular composition, but not molecular complexity or diversity

Brooke E. Propson[1,2], William A. Argiroff[3], Grace A. Cagle[1], Rima A. Upchurch[3], Donald R. Zak[3,4], A. Stuart Grandy[5], and Zachary B. Freedman[1*]

[1]Department of Soil and Environmental Sciences
University of Wisconsin, Madison, WI, USA 53706
[2]University of Michigan Biological Station
9133 Biological Rd, Pellston, MI, USA 49769
[3]School for Environment and Sustainability
[4]Ecology and Evolutionary Biology
University of Michigan, Ann Arbor, MI, USA 48109
[5]Department of Natural Resources and the Environment
University of New Hampshire, Durham, NH, USA 03824

*Corresponding author:
Zachary B. Freedman, zfreedman@wisc.edu (ORCID: 0000-0001-9160-7470)

Abstract

Soil organic matter (SOM) consists of different biochemical constituents that exist across a spectrum of chemical complexity from simple to complex, and the relative abundance of these potential substrates for microbial metabolism can have consequences for the fate of soil C, and consequently the pace of climate change. However, current understanding of the mechanistic controls on SOM biochemistry and decay, and how these may be affected by climate change, is still incomplete. As such, the primary objectives of this study are to assess (1) the trajectory of organic matter decomposition and stabilization from undecayed plant root litter to mineral SOM and (2) how these processes are altered by anthropogenic nitrogen (N) deposition by using high-resolution SOM biochemical and microbiome datasets and a long-term field experiment in the Upper Great Lakes region of North America. N deposition did not significantly alter the biochemical composition of SOM in the undecomposed and 1-year decomposed samples but did alter mineral SOM biochemistry. This shift was attributed to changes in the relative abundance of specific biochemical compounds rather than changes in more broadly defined compound classes, such as lipids, for example. A reduced association between SOM biochemistry and microbial decomposer communities under N deposition was also observed. Taken together, atmospheric N deposition altered the composition of mineral SOM and decoupled the relationship between microbial composition and SOM biochemistry, likely contributing to the previously observed reduction in the decomposition of SOM while not significantly altering SOM's overall biochemistry.

Keywords: SOM, biochemistry, bacteria, fungi, py-GCMS, decomposition

1. Introduction

Soil organic matter (SOM) constitutes the largest terrestrial organic carbon reservoir, and changes in SOM decomposition dynamics under fluctuating environmental conditions could intensify or mitigate impacts of climate change. Inputs from plants, through the deposition of above- and below-ground plant residues and the release of exudates from plant roots represents the largest organic matter input to soils[1,2]. Litter chemical composition, which is often estimated in terms of its nitrogen (N) or lignin contents[3,4], is regarded as one of the primary controls over decomposition rates and SOM accumulation and the fate of these inputs is governed by soil microbial activity[5–9]. In recent decades, there has been a shift from traditional theory of SOM chemical recalcitrance, where biochemically recalcitrant lignified material was thought to constitute the majority of SOM because of its theorized resistance to microbial decomposition[10,11], towards a continuum model of SOM complexity that proposes microbial-derived products as the primary constituents of SOM and the potential importance of molecular diversity in enabling SOM persistence[12–15].

Biochemical compounds that comprise litter exist across a spectrum of chemical complexity from simple to complex substrates and the relative abundance of these potential substrates for microbial metabolism can have consequences for the fate of C stored as mineral SOM[7,14,16]. When plant litter undergoes microbially mediated breakdown during decomposition, the resulting products will differ depending on the initial biochemical quality of the plant litter, as well as the composition of the microbial community decomposing that material[7,17]. The potential importance of biochemical complexity and diversity for SOM persistence lies in the different microbial requirements for metabolizing different biochemical compounds, both for compounds that are structurally dissimilar, as well as ones that are largely similar but may exhibit minor

differences, such as differences in the position of functional groups (for example, *ortho*- versus *para*- benzoic acid)[15,18]. This rise in the acknowledgement and potential importance of a higher resolution understanding of SOM is a deviation from the standard practice in which compounds are typically grouped together as classes (e.g., lipids, etc.) that are assumed to behave similarly through the decomposition process. This results in individual compounds being grouped into classes that are inherently less refined. However, with the conceptual move away from stable SOM largely consisting of recalcitrant material towards a spectrum of which biochemical complexity and diversity enable SOM persistence, research has shown that certain SOM biochemical constituents are resistant to decomposition despite being in a compound class that was traditionally viewed as "labile" (ex: long-chain lipids)[19]. As such, there is increasing emphasis on the potential importance of SOM molecular complexity and diversity in driving SOM persistence[12,15,20–22]. Critically, there is a need to determine how this proposed relationship between SOM molecular diversity and persistence responds to changing climatic conditions.

To better understand how anthropogenic N deposition, a pervasive driver of global environmental change, affects the cycling and storage of SOM, we conducted a 37-year field experiment to simulate future rates of anthropogenic N deposition. After 20 years of experimental N deposition inputs, we found that anthropogenic N deposition slowed the rate and extent of organic matter decomposition, resulting in the accumulation of lignified material in mineral soil derived primarily from fine root litter[23–25]. This change in SOM biochemistry in response to N deposition was associated with decreases in lignolytic fungi and positively associated with saprotrophic bacteria[23,26–28]. However, lignin, and its identifiable derivatives, often comprises ≤10% mineral SOM[19,29–32], meaning a substantial majority of SOM biochemistry has been considered unaltered by N deposition. A higher resolution analysis of SOM chemistry and the soil

90 microbiome through decomposition and N deposition remains a critical gap in our knowledge on
91 the persistence of SOM that built up under anthropogenic N deposition.

92 By using high resolution SOM biochemical and soil microbiome datasets, in the context of
93 a long-term field study, the primary objective of this study was to assess the effect of experimental
94 N deposition on the trajectory of organic matter decomposition and stabilization from undecayed
95 plant root litter to mineral SOM. We assessed the effect of experimental N deposition on SOM
96 molecular abundance, diversity, and complexity during microbial decay by establishing a
97 decomposition gradient from undecomposed fine roots to mineral SOM. Here, we define SOM
98 molecular diversity analogous to species richness and evenness, where molecular richness refers
99 to the number of different biochemical compounds in SOM and molecular evenness describes their
100 relative abundance. We define SOM molecular complexity as how structurally (dis)similar
101 biochemical compounds that constitute SOM are to one another[33]. More molecularly complex
102 SOM would thus have fewer structural similarities between compounds. We hypothesized that
103 experimental N deposition will elicit changes in organic matter biochemistry at the individual
104 compound-level that are not detected when assessed at the less refined compound class-level, and
105 these compound substitutions may have functional implications for storage of SOM in the system.
106 We further hypothesized that changes in SOM biochemistry will be associated with changes in
107 microbial community composition that can explain the observed biochemical changes.
108

109 **2. Methods**

110 **2.1. Description of study sites**

111 The Michigan Nitrogen Deposition Gradient Study was established in 1987 to examine the
112 effects of atmospheric N deposition on ecosystem biogeochemical processes. Spanning a 500-km

113 distance, the study area in Michigan, USA, consists of four replicate sugar maple (*Acer saccharum*)
114 dominated northern hardwood forest stands on sandy spodosol soil (Typic Haplorthods of the
115 Kalkaska series). The stands contain a thick organic horizon that includes a mat of fine roots
116 (Oe/Oa) at its boundary with the A horizon. The stands are floristically and edaphically matched
117 and encompass the full latitudinal range of northern hardwood forests in eastern North America
118 and the Upper Great Lakes Region[34], allowing us to generalize our findings across this widespread
119 ecologically and economically important ecosystem (Table S1). At each site (n = 4), there are six
120 30-m by 30-m plots, three of which received experimental N additions (30 kg NO_3^-N ha^{-1} yr^{-1}) in
121 the form of $NaNO_3$ pellets applied annually in six equal applications throughout the growing
122 season beginning in 1994 and three of which receive ambient atmospheric N deposition (Figure
123 1).

124 **2.2. Field-based experiment, sampling, and sample processing**

125 This field-based experiment was designed to produce samples that constitute a gradient of
126 fine root decomposition, spanning undecomposed fine roots, 1-year decomposed fine roots, and
127 more highly decomposed mineral soil organic matter. To do this, samples were collected in
128 September and October 2013 by collecting soil cores to a depth of 10cm (5-cm-diameter), which
129 included both Oe/Oa and A horizons[23,35]. Cores were transported on ice to the University of
130 Michigan and stored at -20°C. Cores were thawed and passed through a 2mm sieve, and first-
131 through third-order fine roots were collected and pooled at the plot level[36,37]. Roots were rinsed to
132 remove mineral soil and dried at 60°C for 24 hours. The outcome of this processing yielded the
133 "undecomposed" and "mineral SOM" sample fractions (Figure 1). For this purpose, roots from
134 fresh Oe/Oa horizon samples are considered undecomposed in that relative to the other sample
135 types in this experiment, they have undergone decomposition to a lesser degree as indicated by a

136 light coloration and lack of observable decay. Organic material in the mineral soil represents
137 organic matter that has undergone the greatest degree of decomposition and exists as a relatively
138 stable form of SOM compared to organic horizon material[38].

139 To obtain the intermediate, "decomposed" samples, a subset of the undecomposed fine roots
140 from each plot were sterilized and placed in mesh litter bags, deployed in the field, and collected
141 after 12 months. Prior to field incubation, fine roots were sterilized to remove soil microbes using
142 ethylene oxide[39], a process that minimally alters organic matter biochemistry[40], as compared to
143 other methods such as autoclaving[41]. Sterilized fine roots (~2g dry weight) were placed into
144 15x15cm mesh litter bags constructed with 300 µm polyester mesh on top and 20µm polyester
145 mesh on bottom to allow for microfauna and fungal hyphae to enter the bags[35,42]. Litter bags were
146 deployed in their respective plots to their original location in the soil profile at the boundary of the
147 Oe/Oa and A horizons (n = 3 litter bags/plot at 6 plots/site; n = 72 litter bags total). Litter bags
148 were placed in the field in June 2014 and collected in June 2015, immediately storing each bag on
149 ice. The contents of each litter bag were homogenized by hand and composited at the plot level.
150 The decomposed fine root samples were subsampled for biochemical analyses, dried at 60°C for
151 24 hours, and the remaining decomposed fine root material was stored at -80°C for microbial
152 community analyses. Supporting justification and additional details on sample collection and
153 processing can be found in Argiroff et al. (2019)[23].

154 **2.3. Organic matter biochemistry**

155 Subsets of each of the three sample types (undecomposed fine roots, decomposed fine roots,
156 and mineral soil; herein referred to as three different stages of decomposition) were ground with a
157 ball mill and assessed for organic matter biochemistry using pyrolysis-GC/MS[43]. Samples were
158 pyrolyzed at 600°C in quartz tubes for 20 seconds using a DS Pyroprobe 5150 pyrolyzer and

159 analyzed using a ThermoTrace GC Ultra gas chromatograph (Thermo Fisher Scientific, Walthan,
160 MA, USA) and ITQ 900 mass spectrometer (Thermo Fisher Scientific)[23,44] at the University of
161 New Hampshire. Compound peaks were identified and assigned using the Automated Mass
162 Spectral Deconvolution and Identification Systems (AMDIS v2.65) software, the National
163 Institute of Standards and Technology (NIST) compounds library, and published literature[13,43].
164 Organic matter compounds are expressed as the % relative abundance of total sample peak area
165 and classified at the individual compound-level and grouped by compound source origin (e.g.,
166 lignin-derivatives, phenolics, aromatics, proteins, N-bearing, polysaccharides, and lipids).
167 Critically, individual compounds observed in pyrolysis-GC/MS analysis are pyrolysis products of
168 a source compound and are classified according to the nature of their source compound.
169 Identifiable compounds with potentially multiple or unknown origins were classified as
170 unspecified[13]. In total, this effort yielded 260 identifiable compounds, each assigned to one of the
171 8 compound source classes described above (Figure 1).

172 **2.4. Fungal and bacterial community composition**

173 Fungal and bacterial community composition was determined from the remaining subset of
174 decomposed root litter and characterized using ribosomal DNA sequence abundances. Supporting
175 justification and additional details on DNA isolation, PCR amplification, amplicon sequencing,
176 and sequence quality control can be found in Argiroff et al. (2019)[23]. Briefly, total genomic DNA
177 from three replicate subsamples taken from each litter bag was isolated using the DNeasy Plant
178 Mini Kit (Qiagen, Germantown, MD) and checked for quality with a NanoDrop 8000
179 Spectrophotometer (Thermo Scientific) and gel electrophoresis. Replicate extractions from each
180 litter bag were pooled and stored at -80°C prior to PCR amplification. PCR amplification was
181 performed using the LROR and LR3 primers[45] that target the D1-D2 region of the 28S rRNA gene.

182 The V1-V3 regions of the bacterial 16S rRNA gene were targeted using the primers 27f and 519r[46].
183 PCR products were purified using the MinElute PCR Purification Kit (Qiagen) and the quality of
184 the purified PCR products was assessed as described above. Sequencing was performed at the
185 University of Michigan DNA Sequencing Core on 16 SMRT chips with a PacBio RS II system
186 (Pacific Biosciences, Menlo Park, CA). Mean amplicon lengths were 688 bp for fungal 28S and
187 525 bp for bacterial 16S rRNA genes. Sequences were processed using mothur v1.40.5[47]. Fungal
188 sequences were aligned against a 28S reference alignment from the RDP LSU training set[48] and
189 bacterial sequences were aligned against the 16S SILVA v132 reference alignment[49]. Sequences
190 were clustered into operational taxonomic units (OTUs) for fungal and bacterial sequences at 99%
191 and 97% sequence similarity, respectively. The most abundant sequence for each OTU was used
192 as the representative for that OTU, and taxonomic assignments were made using the RDP classifier
193 with the LSU training set v11 for fungi[50] and the SILVA v132 reference alignment with the naïve
194 Bayesian classifier[51] in mothur for bacteria.

195 **2.5. Statistical Analyses**

196 To assess the effect of experimental N deposition on the trajectory of organic matter
197 biochemistry during decay, we assessed compositional change elicited by the treatment in a three-
198 step approach at two increasing levels of biochemical resolution. At the least resolved level, herein
199 referred to as the compound class-level, we used two-way analysis of variance (ANOVA) to test
200 the effect of experimental N deposition, site, and their interaction on $\log_2$-transformed compound
201 class ($n = 8$) abundances for each of the three decomposition stages. At the higher resolution level
202 of analysis, herein referred to as the individual compound-level, we performed PERMANOVA on
203 Euclidean distance matrices of $\log_2$-transformed relative abundances of individual compounds at
204 the three decomposition stages testing for the effect of decomposition stage, treatment, site, and

205 their interactions on organic matter biochemistry. In the case of a significant PERMANOVA
206 outcome, we performed PERMDISP[52] to determine whether this effect was driven by differences
207 in composition, heterogenous variance (i.e., dispersion), or both. The third step in our approach,
208 at the individual compound-level, we additionally performed differential abundance analysis
209 (Wald test)[53,54] to test for the effect of N deposition on individual compound abundances in
210 decomposition stages with a significant PERMANOVA treatment effect.

211 We measured organic matter molecular diversity of each sample (n = 24 per decomposition
212 stage; 72 total) by calculating molecular richness and evenness using the vegan package (v2.6.4)[55]
213 in R and performed two-way ANOVA to test the effect of decomposition stage, N deposition, and
214 their interaction on each molecular diversity metric. When applicable, pairwise comparisons were
215 made using Tukey's honest significant difference test (HSD) to control for multiple comparisons[56].
216 Molecular complexity values were calculated using the Bertz/Hendrickson/Ihlenfeldt formula[57,58]
217 computed by Cactvs 3.4.8.18 (PubChem release 2021.10.14)[59] and are estimates of how
218 complicated a compound's molecular structure is in terms of both the elements contained and
219 structural symmetry. We created molecular networks to represent changes in molecular complexity
220 between compounds present in the ambient and experimental N deposition treatment through
221 decomposition using the chemodiv package (v0.3.0)[33,60] in R and performed ANOVA to test the
222 effect of N deposition on molecular complexity.

223 To assess how experimental N deposition altered microbial community composition and
224 relationships with organic matter biochemistry, we performed Mantel tests on $\log_2$-transformed
225 Euclidean distances of organic matter biochemistry and Hellinger-transformed Bray-Curtis
226 distances of bacterial, fungal, and saprotroph communities (as defined using FUNGuild in R)[61].
227 To determine the taxa that most differed in relative abundance across the decomposition gradient,

228 differential abundance analysis was performed on the bacterial and fungal communities using
229 DESeq2 with *P*-value adjustment for multiple comparisons using the false discovery rate
230 method[62,63].

231 Due to the broad geographic expanse of our experiment and inherent heterogeneity of the
232 soil environment, we accepted statistical significance at $\alpha = 0.1$. All data processing, statistical
233 analyses, and visualizations were performed and produced in R (v4.2.2)[64] and RStudio (version
234 2022.12.0+353)[65], relying extensively on R packages such as vegan (v2.6.4)[55], easyanova
235 (v11.0)[66], and the collection of packages comprising the tidyverse (v1.3.1)[67].

236 **3. Results**

237 **3.1 Compound class biochemistry**

238 At the less-refined compound class-level, experimental N deposition significantly
239 increased the relative abundance of lignin-derived compounds in the mineral SOM (+53%, P =
240 0.09; Figure S1; Table S2) across all sites. However, the experimental N deposition did not affect
241 the abundance of any other compound class at any stage of decomposition (Table S3 and S4).

242 **3.2 Individual compound biochemistry**

243 When assessing the effect of experimental N deposition on the higher resolution, individual
244 compound relative abundances across the three decomposition stages, the composition of
245 individual compounds differed dependent on decomposition stage, site, and the N deposition
246 treatment (decomposition stage × site × treatment; F = 1.29, P = 0.05; Figure 2; Table S5). Pairwise
247 PERMANOVA at each decomposition stage revealed a significant effect of experimental N
248 deposition on mineral SOM biochemistry (F = 4.26, P = 0.004; Figure 2), and no effect on the
249 organic matter biochemistry at the undecomposed (F = 0.18, P = 0.93) or 1-yr decomposed (F =
250 0.20, P = 0.92) stages of decomposition (Table S5). Permutation tests of homogeneity of

multivariate dispersion on the organic matter biochemistry at each of the three decomposition stages were nonsignificant ($P > 0.1$; Table S6), confirming that PERMANOVA detected differences in mineral SOM biochemical composition at the individual compound-level between the ambient and experimental N deposition treatment, rather than detecting changes in variability among samples (i.e., multivariate dispersion). Differential abundance tests of individual compound abundances in mineral SOM revealed that experimental N deposition led to the differential abundance of 19 out of 216 total compounds detected in the mineral SOM (Figure 3). Of these differentially abundant compounds, 7 (3.2% of the total number of compounds) were significantly more abundant in the N deposition treatment and 12 compounds (5.6% of total) were significantly more abundant in the ambient treatment (all $P \leq 0.1$; Table S7). Compounds more abundant under experimental N deposition compared to ambient conditions included: phenol, 3-methyl- (aromatic combustion product), anthracene (aromatic), 4-guaiacylpropane (lignin), benzeneacetic acid, 4-hydroxy-3-methoxy- (lignin), benzene 1-methoxy-4-methyl- (lignin), n-decane (lipid), and 3-pyridinol (N-bearing). Compounds more abundant in the ambient treatment included: benzene 1-ethenyl-4-methoxy- (lignin), propene (lipid), isocrotonic acid (lipid), 3-methylpyridazine (N-bearing), ethanone, 1-(1-methyl-1H-pyrrol-2-yl)- (N-bearing), 2,5-furandione, 3-methyl- (N-bearing), 2(5H)-furanone, 5-methyl- (polysaccharide), 1,2-cyclohexanedione (polysaccharide), acetic anhydride (polysaccharide), benzenepropanenitrile (protein), fluoranthene (unspecified), and (E)-1,3-butadien-1-ol (unspecified).

3.3 Biochemical diversity and complexity

Experimental N deposition did not affect molecular species richness ($F = 0$, $P = 0.97$) or evenness ($F = 0.39$, $P = 0.53$) at any of the three decomposition stages (Figure 4; Table S8). Given the observed treatment differences in biochemical composition in the mineral SOM only, we

assessed the effect of experimental N deposition on molecular complexity at only the mineral SOM decomposition stage. To determine how experimental N deposition affects molecular complexity (i.e., how structurally similar compounds that constitute SOM are to one another), compound co-occurrence and structural dissimilarity matrices were generated for mineral SOM biochemistry in both treatments. Under ambient conditions in the mineral SOM, molecular network analysis revealed 197 nodes, representing compounds, and 2450 edges, representing the structural similarities present between those compounds (Figure 5). Molecular network analysis of the mineral SOM biochemistry in experimental N deposition revealed it did not significantly alter the number of compounds present (n_{nodes} = 187) nor the structural similarities between compounds (n_{edges} = 2502; Figure 5). Molecular complexity values calculated using the Bertz/Hendrickson/Ihlenfeldt formula affirmed that the N deposition treatment did not significantly alter individual compound molecular complexity in the mineral SOM (F = 0, P = 0.997; Figure S2).

Decomposition stage had a significant effect on molecular richness (F = 9.49, P<0.001) and evenness (F = 12.22, P<0.001; Figure 4; Table S8). HSD-adjusted pairwise comparisons revealed significantly higher molecular richness at the 1-yr decomposed stage compared to the undecomposed (post hoc P = 0.001) and mineral SOM (post hoc P<0.001; Figure 4; Table S9). Molecular evenness was significantly higher in the 1-yr decomposed (post hoc P = 0.002) and mineral SOM (post hoc P<0.001) stages of decomposition as compared to the undecomposed root litter (Figure 4; Table S9). There was no difference in molecular evenness between the 1-yr decomposed and mineral SOM decomposition stages (post hoc P = 0.39; Figure 4; Table S9). In the undecomposed root litter, molecular network analysis revealed 209 nodes and 2095 edges, while the 1-yr decomposed root litter network had 225 nodes and 3372 edges, and the mineral

297 SOM network had 216 nodes and 3022 edges (Figure S3). Molecular complexity values calculated
298 using the Bertz/Hendrickson/Ihlenfeldt formula affirmed that decomposition stage did not
299 significantly alter individual compound molecular complexity at any point (F = 0.01, P = 0.99,
300 Figure S4).

301 **3.4 Microbial community associations with SOM biochemistry**

302 Fungal and bacterial communities were differentially associated with organic matter
303 biochemistry at the three decomposition stages in the ambient and N deposition treatments (Figure
304 6). In the ambient treatment, bacterial community composition was significantly correlated with
305 organic matter biochemistry in the undecomposed root litter (R = 0.29, P = 0.07) and weakly
306 associated in the mineral SOM (R = 0.26, P = 0.12) but exhibited no relationship with the organic
307 matter biochemistry in the 1-yr decomposed root litter (Table S10). Under experimental N
308 deposition, bacterial community composition and organic matter biochemistry were not correlated
309 at any of the three decomposition stages. In the ambient treatment, fungal community composition
310 was also not correlated with the 1-yr decomposed root litter (Table S10) and was significantly
311 correlated with the organic matter biochemistry in the mineral SOM (R = 0.20, P = 0.09). Under
312 experimental N deposition, fungal community composition was significantly correlated with the
313 1-yr decomposed root litter biochemistry (R = 0.23, P = 0.04) and marginally associated in the
314 mineral SOM (R = 0.17, P = 0.11) but exhibited no relationship with the organic matter
315 biochemistry in the undecomposed root litter (Table S10; Figure 6). In the ambient treatment,
316 saprotroph community composition was marginally associated with organic matter biochemistry
317 in the undecomposed root litter (R = 0.18, P = 0.15) and significantly correlated with the mineral
318 SOM (R = 0.30, P = 0.06) but exhibited no relationship with the organic matter biochemistry in
319 the 1-yr decomposed root litter (Table S10; Figure 6). Under experimental N deposition,

320 saprotroph community composition and organic matter biochemistry were not correlated at any of
321 the three decomposition stages.

322 The abundances of 28 bacterial OTUs (1.6% of total OTUs) were significantly higher under
323 experimental N deposition as compared to the ambient treatment (Figure S5, Table S11). These
324 OTUs included members of the phylum Bacteroidetes (39%), Proteobacteria (29%),
325 Actinobacteria (14%), Patescibacteria (11%), and Armatimonadetes (7%). Under ambient
326 conditions, 13 bacterial OTUs (0.73% of total OTUs) were present in significantly greater
327 abundance. The phyla included Bacteroidetes (54%), Proteobacteria (38%), and Acidobacteria
328 (8%). The abundances of 14 fungal OTUs (2.6% of total OTUs) were significantly higher under
329 experimental N deposition as compared to the ambient treatment (Figure S5, Table S12). These
330 OTUs included members of the fungal classes Tremellomycetes (42%), Eurotiomycetes (17%),
331 Leotiomycetes (17%), Agaricomycetes (8%), Dothideomycetes (8%), and Sordariomycetes (8%).
332 Under ambient conditions, 2 fungal OTUs (0.43% of total OTUs) were present in significantly
333 greater abundance as compared to the N deposition treatment. The fungal classes include
334 Agaricomycetes (50%) and Sordariomycetes (50%).

335

336 **4. Discussion**

337 **4.1 High resolution molecular analyses reveal N deposition elicits changes to SOM**
338 **biochemistry that were previously undetectable.**

339 It is common to assess SOM biochemistry by grouping individual biochemical compounds
340 into classes, such as lipids or lignin-derived compounds, as a means to simplify biochemical
341 heterogeneity and diversity by grouping compounds that are suspected to behave similarly based
342 on the relative similarity of their structure or other physical properties or factors[12,13,23,68,69]. In doing

343 so, the abundances of individual compounds within a compound class are combined, leading to a
344 loss in the potential resolution of SOM biochemical information, and potentially making impacts
345 of environmental change on SOM biochemical constituents undetectable. As the resolution at
346 which we can examine SOM biochemistry has increased with technological advances, so has the
347 importance in identifying and elucidating the complexity within these traditional compound
348 classes. While it has been common to assume that individual compounds within a class of
349 compounds behave uniformly, there is increasing evidence for contrasting and compounding
350 origins within a compound class and the different potential pathways of mineralization will have
351 implications for the formation and persistence of mineral SOM[2,7,19,20]. As such, the implementation
352 of more refined analytical analyses that aid in elucidating these molecular-level differences can
353 increase understanding of mechanisms governing SOM persistence; a necessary step toward
354 increasing organic matter in soil as a viable climate change mitigation strategy[15,20].

355 To demonstrate this assertion, previous research efforts in this long-term field experiment
356 have detected increases in lignin-derived compounds in mineral SOM under experimental N
357 deposition, with no detectable changes to other components of mineral SOM biochemistry[23,24].
358 However, high resolution analysis used in this study revealed numerous individual compounds
359 changed in mineral SOM within multiple additional compound classes in response to the
360 experimental N deposition that may have consequences for the process of organic matter decay
361 and soil C storage (Figure 3; Table S7). For example, the abundance of lipids in mineral SOM
362 exhibited no effect of experimental N deposition at the compound class-level. However, at the
363 individual compound-level, in the ambient treatment, two molecules that are produced from the
364 combustion of lipids (propene and isocrotonic acid) were 15-times and over 200-times more
365 abundant, respectively, compared to the experimental N deposition treatment (Figure 3; Table S7).

366 Whereas under experimental N deposition, one lipid molecule (n-decane) was over 100-times more
367 abundant compared to in the ambient treatment (Figure 3; Table S7), ultimately leading to no
368 observable effect of the experimental N deposition on the abundance of lipids as a class of
369 compounds (Table S2; Figure S1). This reorganization of individual compounds within compound
370 classes is undetectable by less refined analysis and is critical for understanding the fate of these
371 substrates. Lipids are a highly heterogenous class of compounds with significant input from both
372 plants and soil microbes[70,71]. Though there is rising evidence that stable mineral SOM is largely
373 microbial-derived, it remains unclear and highly context dependent how much is plant-
374 derived[13,19,20,72–75]. Estimations of microbial necromass C in forest soils suggest that a substantial
375 portion (~70%) of C in stabilized SOM could be plant-derived[76,77], and that the contribution of
376 plant-derived lipids to this C pool can be greater than that of lignin[20]. In this study, all three of the
377 differentially abundant lipid molecules across the ambient and experimental N deposition
378 treatments are involved in both plant and microbial metabolic processes[78–80]. As such, more
379 detailed knowledge of the specific metabolic reactions, which plants or microbes are producing
380 them, and how these compounds end up in mineral SOM is necessary to understand the longevity
381 of these substrates in the system[81].

382 Proteins and other N-containing compounds exhibited similar trends at these differing
383 analytical scales. Despite no statistical difference in the abundance of proteins at the compound
384 class-level, at the individual compound-level one protein molecule (benzenepropanenitrile) was
385 almost 8-times more abundant in the ambient treatment compared under experimental N deposition
386 (Figure 3; Table S7). The hydrolysis of benzenepropanenitrile (i.e., 3-phenylpropionitrile) is
387 catalyzed by the nitrilase enzyme (EC 3.5.5.1)[82–85], yielding a carboxylic acid and ammonium
388 (NH_4^+). The gene which encodes the enzyme that ultimately carries out this reaction is found in

389 the genomes of two soil bacteria, one of which being *Paraburkholderia phymatum*[83,86–89]. In this
390 study, *Paraburkholderia spp.* (n = 3; Table S11) were in significantly greater abundance under
391 experimental N deposition compared to the ambient treatment (Figure S4). *Paraburkholderia spp*.
392 are known decomposers in forests, particularly sugar maple forests like the ones in this study[90].
393 Thus, it is plausible that increased enzymatic activity produced by *Paraburkholderia spp.* under
394 experimental N deposition catalyzed this reaction, leading to significantly lower
395 benzenepropanenitrile abundance in the N deposition treatment. These findings suggest that
396 changes to microbial community composition in response to environmental stimuli may have
397 functional consequences and elicit changes to the biochemical composition of organic matter that
398 eventually becomes stable mineral SOM.

399 **4.2 High resolution analysis reveals novel insights into previous findings on lignin**
400 **accumulation in response to N deposition that may underlie resistance to microbial**
401 **decomposition.**

402 In addition to the novel findings detailed above, high resolution analysis of SOM
403 biochemistry revealed additional compositional insight into lignin dynamics in response to the
404 experimental N deposition. Previous work in this long-term experiment showed that anthropogenic
405 N deposition slowed the rate and extent of organic matter decomposition, ultimately resulting in
406 the accumulation of lignified material in mineral SOM under experimental N deposition (+53%,
407 P = 0.09; Figure S1; Table S2)[23–25,28]. However, at the individual compound-level, changes in the
408 composition of lignin compounds in mineral SOM were detected under both ambient and
409 experimental N deposition conditions. In the ambient treatment, one lignin-derived molecule
410 (benzene, 1-ethenyl-4-methoxy-) was almost 8-times more abundant compared to under
411 experimental N deposition (Figure 3; Table S7). Whereas under experimental N deposition, three

412 different lignin-derived molecules (benzene, 1-methoxy-4-methyl-, homovanillic acid, and 4-
413 guaiacylpropane) were 8-times, 14-times, and 29-times more abundant than in the ambient
414 treatment, respectively, ultimately leading to the overall increase observed at the compound class-
415 level (Figure 3; Figure S1; Table S7).

416 At the relatively less-refined compound class-level, it is not possible to detect this
417 reorganization of different lignin molecules, as observed here, that ultimately affects the
418 interpretability of the stability of the compound class as a whole. Lignin is a complex
419 macromolecule that is highly variable in terms of its primary structure. Which lignin monomers
420 and functional groups are present, in what quantities, and what linkages connect them affect the
421 decomposability of lignin polymers by soil microbes[91–94]. For example, lignin polymers containing
422 higher quantities of monomers of the guaiacyl (G) subunit are more resistant to decomposition,
423 resulting in significantly lower mass loss, than lignin polymers composed of other subunits[16,93].
424 The 29-times greater abundance of 4-guaiacylpropane and 14-times greater abundance of
425 homovanillic acid, a G subunit decomposition product[95], under experimental N deposition suggests
426 that the SOM that has accumulated under anthropogenic N deposition is particularly
427 compositionally resistant to microbial decomposition in terms of its lignin content. Thus, it is
428 plausible that in this system, differences in the quality of lignin, in addition to the increases in
429 lignin quantity[23], may be a factor contributing to the increased SOM observed under high N
430 deposition conditions.

431 Differences in the composition of decomposing microbial communities observed under
432 experimental N deposition support the claim that lignin in mineral SOM under increased
433 anthropogenic N deposition is particularly resistant to decomposition or is simply not being
434 metabolized by the microbial community in this treatment. While fungi are widely considered as

435 primary lignin decomposers, evidence has shown that bacteria may play a non-inconsequential
436 role in lignin decay[96,97]. Of the bacterial OTUs in higher abundance under N deposition conditions,
437 just under half (43%) belong to the phyla Proteobacteria and Actinobacteria (Figure S4; Table
438 S11). This finding aligns with previous work in this system that observed an increase in the
439 abundance of bacteria associated with lignin decay under experimental N deposition[26,27]. The
440 majority of lignin-degrading bacteria identified to date represent three bacterial classes, all which
441 are within the Proteobacteria and Actinobacteria phyla: Actinomycetes, α-Proteobacteria, and γ-
442 Proteobacteria[98–100]. Such bacteria capable of lignin degradation do so in an incomplete manner,
443 such that smaller aromatic lignin-derived compounds are produced[101–103]. Thus, it is plausible that
444 the accumulation of decomposition resistant lignin material under experimental N deposition was
445 due, in part, to the incomplete bacterial metabolism of lignin and the inability to break down these
446 compounds specifically.

447 **4.3 Molecular complexity and diversity are not drivers of SOM persistence in this system.**

448 In this study, despite the above-described differences observed at the individual compound-
449 level, we did not detect overall difference in the molecular complexity of SOM between the
450 undecomposed root litter, 1-year decomposed root litter, and mineral SOM (Figure S3). This
451 finding indicates that although the composition of the individual compounds changed during decay
452 (Figure 2), the molecular complexity (i.e., structural [dis]similarity) of the compounds that
453 constitute SOM at a given stage of decomposition did not (Figure 2; Figure S3). This finding
454 differs from both what has been proposed conceptually about organic matter complexity
455 underlying SOM persistence[15] and from recent studies that have found the opposite: that persistent
456 SOM is less complex than its initial inputs[12,21,104]. In this system, the lack of relationship between
457 SOM molecular complexity and persistence may be attributable to site-specific factors or

458 differences in the physiological capacity of the active microbial community. The soils in our
459 experiment are sandy (~85%) spodosols and thus chemical sorption to mineral soil particles is a
460 less prominent mechanism of SOM persistence[20]. Molecular complexity may be a more important
461 indicator for soils with greater clay content and thus higher matrix stabilization potential.

462 In contrast to SOM molecular complexity, SOM diversity (i.e., molecular richness and
463 evenness) did change throughout decomposition (Figure 4). Both molecular richness and evenness
464 were higher after one year of decomposition compared to initial undecomposed inputs (Figure 4;
465 Table S9). This is likely the result of the production of microbially-derived compounds during the
466 initial phases of root decay. When microbes break down plant litter, new byproducts are
467 produced[7,13,105], which likely explains the observed increases in molecular richness, i.e., the
468 number of compounds present, after one year of decomposition. Molecular richness of mineral
469 SOM returning to the same levels as initial inputs may indicate the complete decay of more
470 accessible components of litter or that the microbially processed C substrates that were produced
471 during one year of decomposition were similarly consumed, returning to the same number of
472 compounds as initial inputs, though the composition of those compounds are distinct (Figure 2;
473 Figure 4).

474 **4.4 N deposition decouples relationships between SOM and decomposing microbes,**
475 **potentially reflecting interactions between energetics and nutrient availability.**

476 The bacterial and saprotrophic fungal communities exhibit strong relationships with the
477 biochemistry of the organic matter in the undecomposed litter and mineral SOM under ambient
478 conditions (Figure 6; Table S10). Yet, under experimental N deposition these relationships are
479 lost. The expression of microbial genes and the subsequent production of extracellular enzymes
480 that govern the breakdown of SOM are highly sensitive to N additions[28,106–109]. Under high N

481 conditions, genes responsible for the production of extracellular enzymes that break down complex
482 macromolecules, such as lignin, are downregulated[28]. Additional studies have observed a shift in
483 microbial community composition under N deposition conditions towards a community whose
484 primary niche is the decay of simpler compounds, such as cellulose[106,110,111]. Taken together, it is
485 plausible that when N is readily available, microbes do not need to expend the energy producing
486 extracellular enzymes to break down organic material and this decreased activity may result in a
487 shift in the community composition. This lack of microbial activity may explain why we observed
488 a decoupling of SOM biochemistry and the microbial community composition under experimental
489 N deposition.

490 **4.5 Conclusions and implications**

491 Our results demonstrate that N deposition altered the abundance of specific compounds in
492 mineral SOM, a reorganization of SOM biochemistry that is not detectable when assessing changes
493 at the less-refined compound class-level, as well as decoupled the relationship between microbial
494 composition and SOM biochemistry. Whether these observed changes have functional
495 implications for the long-term storage of SOM is unknown and warrants further investigation.
496 Though these molecular-level differences in SOM biochemistry under anthropogenic N deposition
497 may appear subtle, the effect that these differences have on the C stored in the system long-term
498 may be disproportionately large. For example, in this system, upon termination of the experimental
499 N deposition, a globally ecologically relevant environmental change in response to Clean Air Act
500 Amendments, microbial activity significantly increased and the C that built up under experimental
501 N deposition was lost from the system within 5-years of treatment termination[38]. Studies have
502 shown that molecular-level changes in SOM biochemistry, in response to various environmental
503 change conditions, impact the capacity of temperate forests to sequester C[112]. A microbial

mechanism may underlie this possibility as differences in the structural properties of the molecules in greater abundance under anthropogenic N deposition may have implications for how and by whom these products are transformed, what products are produced, and, ultimately, the decomposability of their byproducts[80,113,114]. Taken together, it is plausible that the SOM that accumulated under experimental N deposition was molecularly distinct as a result of functional changes in the microbial community elicited by the N deposition treatment[23,28]. Thus, upon termination of experimental N deposition, the accumulated, molecularly distinct SOM may have been readily decomposed by the active microbial community upon return to low (i.e., ambient) N conditions. By analyzing SOM biochemistry at more refined analytical scales, we were able to elucidate the mechanisms underlying this system's fluctuating soil C dynamics in response to ongoing environmental change.

Author Contributions

D.R.Z. designed the study. R.A.U. and W.A.A. performed field and laboratory analyses. A.S.G. performed biochemical analyses. B.E.P. analyzed the data with the help of G.A.C. B.E.P wrote the first draft of the manuscript. D.R.Z., W.A.A., G.A.C., and Z.B.F. provided significant feedback on subsequent versions and analyses.

Acknowledgements

We thank Annalisa Stevenson for her help in ArcGIS. We also wish to thank Thea Whitman (and lab), Erika Marín-Spiotta (and lab), the Department of Soil and Environmental Sciences graduate students, and the anonymous reviewers for their thoughtful feedback on this work. This material is based upon work supported by the National Science Foundation Graduate Research Fellowship Program under Grant No. DGE-2137424 awarded to B.E.P. and from the United States Department of Energy Biological Environmental Research program. The maintenance of our long-

term field experiment is supported by the National Science Foundation Long-Term Research in Environmental Biology program.

References

1. Bowden, R. D. *et al.* Litter Input Controls on Soil Carbon in a Temperate Deciduous Forest. *Soil Sci. Soc. Am. J.* **78**, (2014).
2. Cotrufo, M. F. & Lavallee, J. M. Soil organic matter formation, persistence, and functioning: A synthesis of current understanding to inform its conservation and regeneration. in *Advances in Agronomy* vol. 172 1–66 (Elsevier, 2022).
3. Jenkinson, D. S. & Rayner, J. H. THE TURNOVER OF SOIL ORGANIC MATTER IN SOME OF THE ROTHAMSTED CLASSICAL EXPERIMENTS: *Soil Sci.* **123**, 298–305 (1977).
4. Parton, W. J., Schimel, D. S., Cole, C. V. & Ojima, D. S. Analysis of Factors Controlling Soil Organic Matter Levels in Great Plains Grasslands. *Soil Sci. Soc. Am. J.* **51**, 1173–1179 (1987).
5. Adair, E. C. *et al.* Simple three-pool model accurately describes patterns of long-term litter decomposition in diverse climates. *Glob. Change Biol.* **14**, 2636–2660 (2008).
6. Berg, B. & Meentemeyer, V. Litter quality in a north European transect versus carbon storage potential. *Plant Soil* **242**, 83–92 (2002).
7. Cotrufo, M. F., Wallenstein, M. D., Boot, C. M., Denef, K. & Paul, E. The Microbial Efficiency-Matrix Stabilization (MEMS) framework integrates plant litter decomposition with soil organic matter stabilization: do labile plant inputs form stable soil organic matter? *Glob. Change Biol.* **19**, 988–995 (2013).
8. Prescott, C. E. Litter decomposition: what controls it and how can we alter it to sequester more carbon in forest soils? *Biogeochemistry* **101**, 133–149 (2010).
9. Zhang, D., Hui, D., Luo, Y. & Zhou, G. Rates of litter decomposition in terrestrial ecosystems: global patterns and controlling factors. *J. Plant Ecol.* **1**, 85–93 (2008).

10. Berg, B. & McClaugherty, C. *Plant Litter*. (Springer Berlin Heidelberg, Berlin, Heidelberg, 2008). doi:10.1007/978-3-540-74923-3.

11. Waksman, S. A. Humus Origin, Chemical Composition, and Importance in Nature. *Soil Science* **41**, (1936).

12. Jones, A. R. *et al.* Molecular complexity and diversity of persistent soil organic matter. *Soil Biol. Biochem.* **184**, 109061 (2023).

13. Kallenbach, C. M., Frey, S. D. & Grandy, A. S. Direct evidence for microbial-derived soil organic matter formation and its ecophysiological controls. *Nat. Commun.* 10 (2016).

14. Lehmann, J. & Kleber, M. The contentious nature of soil organic matter. *Nature* **528**, 60–68 (2015).

15. Lehmann, J. *et al.* Persistence of soil organic carbon caused by functional complexity. *Nat. Geosci.* **13**, 529–534 (2020).

16. Talbot, J. M., Yelle, D. J., Nowick, J. & Treseder, K. K. Litter decay rates are determined by lignin chemistry. *Biogeochemistry* **108**, 279–295 (2012).

17. Wickings, K., Grandy, A. S., Reed, S. C. & Cleveland, C. C. The origin of litter chemical complexity during decomposition. *Ecol. Lett.* **15**, 1180–1188 (2012).

18. Sugai, S. F. & Schimel, J. P. Decomposition and biomass incorporation of 14c-labeled glucose and phenolics in taiga forest floor: effect of substrate quality, successional state, and season. *Soil Biol. Biochem.* **25**, 1379–1389 (1993).

19. Whalen, E. D. *et al.* Clarifying the evidence for microbial- and plant-derived soil organic matter, and the path toward a more quantitative understanding. *Glob. Change Biol.* gcb.16413 (2022) doi:10.1111/gcb.16413.

20. Angst, G., Mueller, K. E., Nierop, K. G. J. & Simpson, M. J. Plant- or microbial-derived? A review on the molecular composition of stabilized soil organic matter. *Soil Biol. Biochem.* **156**, 108189 (2021).

21. Davenport, R. *et al.* Decomposition decreases molecular diversity and ecosystem similarity of soil organic matter. *Proc. Natl. Acad. Sci.* **120**, e2303335120 (2023).

22. Yang, S. *et al.* Soil organic carbon content and mineralization controlled by the composition, origin and molecular diversity of organic matter: A study in tropical alpine grasslands. *Soil Tillage Res.* **215**, 105203 (2022).

23. Argiroff, W. A., Zak, D. R., Upchurch, R. A., Salley, S. O. & Grandy, A. S. Anthropogenic N deposition alters soil organic matter biochemistry and microbial communities on decaying fine roots. *Glob. Change Biol.* **25**, 4369–4382 (2019).

24. Zak, D. R., Holmes, W. E., Burton, A. J., Pregitzer, K. S. & Talhelm, A. F. SIMULATED ATMOSPHERIC NO_3^- DEPOSITION INCREASES SOIL ORGANIC MATTER BY SLOWING DECOMPOSITION. *Ecol. Appl.* **18**, 2016–2027 (2008).

25. Whittinghill, K. A., Currie, W. S., Zak, D. R., Burton, A. J. & Pregitzer, K. S. Anthropogenic N Deposition Increases Soil C Storage by Decreasing the Extent of Litter Decay: Analysis of Field Observations with an Ecosystem Model. *Ecosystems* **15**, 450–461 (2012).

26. Freedman, Z. & Zak, D. R. Atmospheric N Deposition Increases Bacterial Laccase-Like Multicopper Oxidases: Implications for Organic Matter Decay. *Appl. Environ. Microbiol.* **80**, 4460–4468 (2014).

27. Freedman, Z. B., Upchurch, R. A. & Zak, D. R. Microbial Potential for Ecosystem N Loss Is Increased by Experimental N Deposition. *PLOS ONE* **11**, e0164531 (2016).

28. Zak, D. R. *et al.* Anthropogenic N deposition, fungal gene expression, and an increasing soil carbon sink in the Northern Hemisphere. *Ecology* **100**, (2019).

29. Angst, G., Mueller, K. E., Kögel-Knabner, I., Freeman, K. H. & Mueller, C. W. Aggregation controls the stability of lignin and lipids in clay-sized particulate and mineral associated organic matter. *Biogeochemistry* **132**, 307–324 (2017).

30. Bol, R., Poirier, N., Balesdent, J. & Gleixner, G. Molecular turnover time of soil organic matter in particle-size fractions of an arable soil. *Rapid Commun. Mass Spectrom.* **23**, 2551–2558 (2009).

31. Geng, J. *et al.* Different Molecular Characterization of Soil Particulate Fractions under N Deposition in a Subtropical Forest. *Forests* **10**, 914 (2019).

32. Grandy, A. S. & Neff, J. C. Molecular C dynamics downstream: The biochemical decomposition sequence and its impact on soil organic matter structure and function. *Sci. Total Environ.* **404**, 297–307 (2008).

33. Petrén, H., Köllner, T. G. & Junker, R. R. Quantifying chemodiversity considering biochemical and structural properties of compounds with the R package CHEMODIV. *New Phytol.* **237**, 2478–2492 (2023).

34. Burton, A. J., Ramm, C. W., Pregitzer, K. S. & Reed, D. D. Use of multivariate methods in forest research site selection. *Can. J. For. Res.* **21**, 1573–1580 (1991).

35. Xia, M., Talhelm, A. F. & Pregitzer, K. S. Long-Term Simulated Atmospheric Nitrogen Deposition Alters Leaf and Fine Root Decomposition. *Ecosystems* **21**, 1–14 (2018).

36. Pregitzer, K. S. *et al.* FINE ROOT ARCHITECTURE OF NINE NORTH AMERICAN TREES. *Ecol. Monogr.* **72**, 293–309 (2002).

619 37. Xia, M., Talhelm, A. F. & Pregitzer, K. S. Fine roots are the dominant source of
620 recalcitrant plant litter in sugar maple-dominated northern hardwood forests. *New Phytol.* **208**,
621 715–726 (2015).
622 38. Propson, B. E., Zak, D. R., Classen, A. T., Burton, A. J. & Freedman, Z. B. Gains in soil
623 carbon storage under anthropogenic nitrogen deposition are rapidly lost following its
624 cessation. *Ecology* **105**, e4444 (2024).
625 39. Rose, R. E. & Bailey, R. W. Ethylene Oxide for Soil Sterilization. *Nature* **169**, 716–716
626 (1952).
627 40. Gennari, M., Negre, M. & Ambrosoli, R. Effects of ethylene oxide on soil microbial
628 content and some soil chemical characteristics. *Plant Soil* **102**, 197–200 (1987).
629 41. Berns, A. E. *et al.* Effect of gamma-sterilization and autoclaving on soil organic matter
630 structure as studied by solid state NMR, UV and fluorescence spectroscopy. *Eur. J. Soil Sci.*
631 **59**, 540–550 (2008).
632 42. Hobbie, S. E. Contrasting Effects of Substrate and Fertilizer Nitrogen on the Early Stages
633 of Litter Decomposition. *Ecosystems* **8**, 644–656 (2005).
634 43. Grandy, A. S., Strickland, M. S., Lauber, C. L., Bradford, M. A. & Fierer, N. The
635 influence of microbial communities, management, and soil texture on soil organic matter
636 chemistry. *Geoderma* **150**, 278–286 (2009).
637 44. Pold, G., Grandy, A. S., Melillo, J. M. & DeAngelis, K. M. Changes in substrate
638 availability drive carbon cycle response to chronic warming. *Soil Biol. Biochem.* **110**, 68–78
639 (2017).

640 45. Vilgalys, R. & Hester, M. Rapid genetic identification and mapping of enzymatically
641 amplified ribosomal DNA from several Cryptococcus species. *J. Bacteriol.* **172**, 4238–4246
642 (1990).
643 46. Lane, D. J. 16S/23S rRNA sequencing. *Nucleic acid techniques in bacterial systematics*
644 (1991).
645 47. Schloss, P. D. *et al.* Introducing mothur: Open-Source, Platform-Independent,
646 Community-Supported Software for Describing and Comparing Microbial Communities.
647 *Appl. Environ. Microbiol.* **75**, 7537–7541 (2009).
648 48. Mueller, R. C., Balasch, M. M. & Kuske, C. R. Contrasting soil fungal community
649 responses to experimental nitrogen addition using the large subunit rRNA taxonomic marker
650 and cellobiohydrolase I functional marker. *Mol. Ecol.* **23**, 4406–4417 (2014).
651 49. Quast, C. *et al.* The SILVA ribosomal RNA gene database project: improved data
652 processing and web-based tools. *Nucleic Acids Res.* **41**, D590–D596 (2012).
653 50. Cole, J. R. *et al.* Ribosomal Database Project: data and tools for high throughput rRNA
654 analysis. *Nucleic Acids Res.* **42**, D633–D642 (2014).
655 51. Wang, Q., Garrity, G. M., Tiedje, J. M. & Cole, J. R. Naïve Bayesian Classifier for Rapid
656 Assignment of rRNA Sequences into the New Bacterial Taxonomy. *Appl. Environ. Microbiol.*
657 **73**, 5261–5267 (2007).
658 52. Anderson, M. J. PERMANOVA_2factor: a FORTRAN computer program for
659 permutational multivariate analysis of variance (for any two-factor ANOVA design) using
660 permutation tests. *Department of Statistics, University of Auckland, Auckland* 35 (2004).

661 53. Langley, S. R. & Mayr, M. Comparative analysis of statistical methods used for detecting
662 differential expression in label-free mass spectrometry proteomics. *J. Proteomics* **129**, 83–92
663 (2015).
664 54. Yang, L. & Chen, J. A comprehensive evaluation of microbial differential abundance
665 analysis methods: current status and potential solutions. *Microbiome* **10**, 130 (2022).
666 55. Oksanen, J. *et al.* vegan: Community Ecology Package. 2.7–1
667 https://doi.org/10.32614/CRAN.package.vegan (2001).
668 56. Yandell, B. S. *Practical Data Analysis for Designed Experiments*. (Routledge, 1997).
669 doi:10.1201/9780203742563.
670 57. Bertz, S. H. The first general index of molecular complexity. *J. Am. Chem. Soc.* **103**,
671 3599–3601 (1981).
672 58. Hendrickson, J. B., Huang, P. & Toczko, A. G. Molecular complexity: a simplified
673 formula adapted to individual atoms. *J. Chem. Inf. Comput. Sci.* **27**, 63–67 (1987).
674 59. Kim, S. *et al.* PubChem 2025 update. *Nucleic Acids Res.* **53**, D1516–D1525 (2025).
675 60. Petrén, H., Köllner, T. G. & Junker, R. R. chemodiv: Analysing Chemodiversity of
676 Phytochemical Data. 0.3.1 https://doi.org/10.32614/CRAN.package.chemodiv (2022).
677 61. Nguyen, N. H. *et al.* FUNGuild: An open annotation tool for parsing fungal community
678 datasets by ecological guild. *Fungal Ecol.* **20**, 241–248 (2016).
679 62. Benjamini, Y. & Hochberg, Y. Controlling the false discovery rate: a practical and
680 powerful approach to multiple testing. *Journal of the Royal statistical society: series B* **57**,
681 289–300 (1995).
682 63. Love, M. I., Huber, W. & Anders, S. Moderated estimation of fold change and dispersion
683 for RNA-seq data with DESeq2. *Genome Biol.* **15**, 550 (2014).

64. R Core Team. R: A Language and Environment for Statistical Computing. R Foundation for Statistical Computing (2022).

65. RStudio Team. RStudio: Integrated development environment for R. (2022).

66. Arnhold, E. easyanova: Analysis of Variance and Other Important Complementary Analyses. 11.0 https://doi.org/10.32614/CRAN.package.easyanova (2012).

67. Wickham, H. *et al.* Welcome to the Tidyverse. *J. Open Source Softw.* **4**, 1686 (2019).

68. Geng, J., Fang, H., Cheng, S. & Pei, J. Effects of N deposition on the quality and quantity of soil organic matter in a boreal forest: Contrasting roles of ammonium and nitrate. *CATENA* **198**, 104996 (2021).

69. Sanderman, J. & Grandy, A. S. Ramped thermal analysis for isolating biologically meaningful soil organic matter fractions with distinct residence times. *SOIL* **6**, 131–144 (2020).

70. Arteaga-Clemente, G., García-González, M. A. & González-González, M. Soil lipid analysis by chromatography: A critical review of the current state in sample preparation. *J. Chromatogr. Open* **6**, 100173 (2024).

71. Dinel, H., Schnitzer, M. & Mehuys, G. R. Soil Lipids: Origin, Nature, Content, Decomposition, and Effect on Soil Physical Properties. in *Soil Biochemistry* 397–430 (Routledge, 2017). doi:10.1201/9780203739389-8.

72. Kindler, R., Miltner, A., Thullner, M., Richnow, H.-H. & Kästner, M. Fate of bacterial biomass derived fatty acids in soil and their contribution to soil organic matter. *Org. Geochem.* **40**, 29–37 (2009).

73. Miltner, A., Bombach, P., Schmidt-Brücken, B. & Kästner, M. SOM genesis: microbial biomass as a significant source. *Biogeochemistry* **111**, 41–55 (2012).

74. Olivelli, M. S. *et al.* Unraveling Mechanisms behind Biomass–Clay Interactions Using Comprehensive Multiphase Nuclear Magnetic Resonance (NMR) Spectroscopy. *ACS Earth Space Chem.* **4**, 2061–2072 (2020).

75. Rempfert, K. R. *et al.* Biomolecular budget of persistent, microbial-derived soil organic carbon: The importance of underexplored pools. *Sci. Total Environ.* **932**, 172916 (2024).

76. Khan, K. S., Mack, R., Castillo, X., Kaiser, M. & Joergensen, R. G. Microbial biomass, fungal and bacterial residues, and their relationships to the soil organic matter C/N/P/S ratios. *Geoderma* **271**, 115–123 (2016).

77. Liang, C., Amelung, W., Lehmann, J. & Kästner, M. Quantitative assessment of microbial necromass contribution to soil organic matter. *Glob. Change Biol.* **25**, 3578–3590 (2019).

78. Fahy, E. *et al.* Update of the LIPID MAPS comprehensive classification system for lipids. *J. Lipid Res.* **50**, S9–S14 (2009).

79. Liebisch, G. *et al.* Update on LIPID MAPS classification, nomenclature, and shorthand notation for MS-derived lipid structures. *J. Lipid Res.* **61**, 1539–1555 (2020).

80. Tian, Z. *et al.* PMhub 1.0: a comprehensive plant metabolome database. *Nucleic Acids Res.* **52**, D1579–D1587 (2024).

81. Klier, K. M. & Anantharaman, K. An updated view of metabolic handoffs in microbiomes. *Trends Microbiol.* S0966842X25002203 (2025) doi:10.1016/j.tim.2025.07.009.

82. Harper, D. B. Microbial metabolism of aromatic nitriles. Enzymology of C–N cleavage by *Nocardia* sp. (*Rhodochrous* group) N.C.I.B. 11216. *Biochem. J.* **165**, 309–319 (1977).

728 83. Howden, A. J. M., Rico, A., Mentlak, T., Miguet, L. & Preston, G. M. *Pseudomonas*
729 *syringae* pv. *syringae* B728a hydrolyses indole-3-acetonitrile to the plant hormone indole-3-
730 acetic acid. *Mol. Plant Pathol.* **10**, 857–865 (2009).
731 84. Thimann, K. V. & Mahadevan, S. Nitrilase. *Arch. Biochem. Biophys.* **105**, 133–141
732 (1964).
733 85. Pace, H. C. & Brenner, C. The nitrilase superfamily: classification, structure and
734 function. *Genome Biol.* **2**, reviews0001.1 (2001).
735 86. Bessonnet, T. *et al.* Purification and Characterization of Nitphym, a Robust Thermostable
736 Nitrilase From Paraburkholderia phymatum. *Front. Bioeng. Biotechnol.* **9**, 686362 (2021).
737 87. Moulin, L. *et al.* Complete Genome sequence of Burkholderia phymatum STM815T, a
738 broad host range and efficient nitrogen-fixing symbiont of Mimosa species. *Stand. Genomic*
739 *Sci.* **9**, 763–774 (2014).
740 88. Teepakorn, C. *et al.* Nitrilase immobilization and transposition from a micro-scale batch
741 to a continuous process increase the nicotinic acid productivity. *Biotechnol. J.* **16**, 2100010
742 (2021).
743 89. Vergne-Vaxelaire, C. *et al.* Nitrilase Activity Screening on Structurally Diverse
744 Substrates: Providing Biocatalytic Tools for Organic Synthesis. *Adv. Synth. Catal.* **355**, 1763–
745 1779 (2013).
746 90. Wilhelm, R. C., DeRito, C. M., Shapleigh, J. P., Madsen, E. L. & Buckley, D. H.
747 Phenolic acid-degrading *Paraburkholderia* prime decomposition in forest soil. *ISME*
748 *Commun.* **1**, 4 (2021).

749 91. Bhatnagar, J. M., Peay, K. G. & Treseder, K. K. Litter chemistry influences
750 decomposition through activity of specific microbial functional guilds. *Ecol. Monogr.* **88**,
751 429–444 (2018).
752 92. Pisani, O., Frey, S. D., Simpson, A. J. & Simpson, M. J. Soil warming and nitrogen
753 deposition alter soil organic matter composition at the molecular-level. *Biogeochemistry* **123**,
754 391–409 (2015).
755 93. Thirunavukkarasu, A. *et al.* Unraveling the dynamics of lignin chemistry on
756 decomposition to understand its contribution to soil organic matter accumulation. *Plant Soil*
757 (2024) doi:10.1007/s11104-024-07066-y.
758 94. vandenEnden, L. *et al.* Molecular-level changes in soil organic matter composition after
759 10 years of litter, root and nitrogen manipulation in a temperate forest. *Biogeochemistry* **141**,
760 183–197 (2018).
761 95. Alruwaili, A. *et al.* Elucidation of microbial lignin degradation pathways using synthetic
762 isotope-labelled lignin. *RSC Chem. Biol.* **4**, 47–55 (2023).
763 96. DeAngelis, K. M. *et al.* Characterization of Trapped Lignin-Degrading Microbes in
764 Tropical Forest Soil. *PLoS ONE* **6**, e19306 (2011).
765 97. DeAngelis, K. M. *et al.* Evidence supporting dissimilatory and assimilatory lignin
766 degradation in Enterobacter lignolyticus SCF1. *Front. Microbiol.* **4**, (2013).
767 98. Bugg, T. D. H., Ahmad, M., Hardiman, E. M. & Rahmanpour, R. Pathways for
768 degradation of lignin in bacteria and fungi. *Nat. Prod. Rep.* **28**, 1883 (2011).
769 99. Janusz, G. *et al.* Lignin degradation: microorganisms, enzymes involved, genomes
770 analysis and evolution. *FEMS Microbiol. Rev.* **41**, 941–962 (2017).

771 100. Lee, S., Kang, M., Bae, J.-H., Sohn, J.-H. & Sung, B. H. Bacterial Valorization of Lignin:
772 Strains, Enzymes, Conversion Pathways, Biosensors, and Perspectives. *Front. Bioeng.*
773 *Biotechnol.* **7**, 209 (2019).
774 101. Bugg, T. D., Ahmad, M., Hardiman, E. M. & Singh, R. The emerging role for bacteria in
775 lignin degradation and bio-product formation. *Curr. Opin. Biotechnol.* **22**, 394–400 (2011).
776 102. Granja-Travez, R. S., Persinoti, G. F., Squina, F. M. & Bugg, T. D. H. Functional
777 genomic analysis of bacterial lignin degraders: diversity in mechanisms of lignin oxidation
778 and metabolism. *Appl. Microbiol. Biotechnol.* **104**, 3305–3320 (2020).
779 103. Gu, J. *et al.* Bacterial transformation of lignin: key enzymes and high-value products.
780 *Biotechnol. Biofuels Bioprod.* **17**, 2 (2024).
781 104. Zhang, Z. *et al.* Changes in molecular composition, diversity, and network complexity of
782 soil organic carbon along the elevation in Changbai Mountain, Northeast China. *Geoderma*
783 **443**, 116842 (2024).
784 105. Prescott, C. E. & Vesterdal, L. Decomposition and transformations along the continuum
785 from litter to soil organic matter in forest soils. *For. Ecol. Manag.* **498**, 119522 (2021).
786 106. Frey, S. D., Knorr, M., Parrent, J. L. & Simpson, R. T. Chronic nitrogen enrichment
787 affects the structure and function of the soil microbial community in temperate hardwood and
788 pine forests. *For. Ecol. Manag.* **196**, 159–171 (2004).
789 107. Hesse, C. N. *et al.* Forest floor community metatranscriptomes identify fungal and
790 bacterial responses to N deposition in two maple forests. *Front. Microbiol.* **6**, (2015).
791 108. Li, X. *et al.* Nitrogen addition restricts key soil ecological enzymes and nutrients by
792 reducing microbial abundance and diversity. *Sci. Rep.* **15**, 5560 (2025).

109. Moore, J. A. M. *et al.* Fungal community structure and function shifts with atmospheric nitrogen deposition. *Glob. Change Biol.* **27**, 1349–1364 (2021).

110. Frey, S. D. *et al.* Chronic nitrogen additions suppress decomposition and sequester soil carbon in temperate forests. *Biogeochemistry* **121**, 305–316 (2014).

111. Van Diepen, L. T. A., Frey, S. D., Landis, E. A., Morrison, E. W. & Pringle, A. Fungi exposed to chronic nitrogen enrichment are less able to decay leaf litter. *Ecology* **98**, 5–11 (2017).

112. Castañeda-Gómez, L. *et al.* Soil organic matter molecular composition with long-term detrital alterations is controlled by site-specific forest properties. *Glob. Change Biol.* gcb.16456 (2022) doi:10.1111/gcb.16456.

113. Bossio, D. A. *et al.* The role of soil carbon in natural climate solutions. *Nat. Sustain.* **3**, 391–398 (2020).

114. Crow, S. E. *et al.* Sources of plant-derived carbon and stability of organic matter in soil: implications for global change. *Glob. Change Biol.* **15**, 2003–2019 (2009).

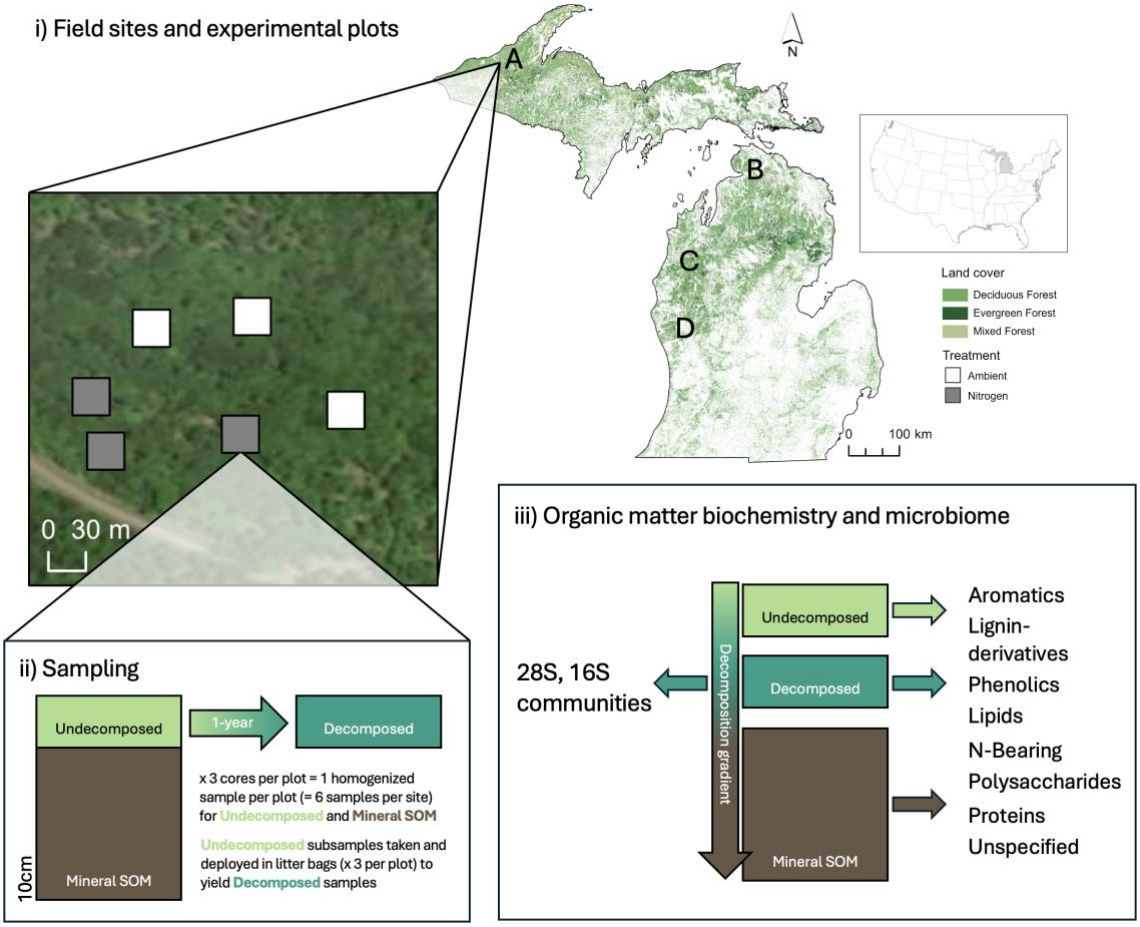

Figure 1. The distribution of study sites in Michigan, USA that span the geographic range of northern hardwood forests. At each site (n = 4), there are six 30 m x 30 m plots, three of which received annual experimental nitrogen (N) additions in the form of 30 kg NO_3^-N ha^{-1} yr^{-1} beginning in 1994 and three of which receive ambient atmospheric N deposition (i). Maps created using ArcGIS Pro: release 3.3.1 (2024; Dewitz, 2021). Cores were collected (n = 3 per plot) to yield the undecomposed and mineral SOM samples. Subsets of undecomposed material were deployed in litter bags and left to decompose for 1-year to yield the decomposed samples (ii). The biochemistry of all three sample types was assessed using pyrolysis-GC/MS and bacterial and fungal community composition was determined on the decomposed samples (iii).

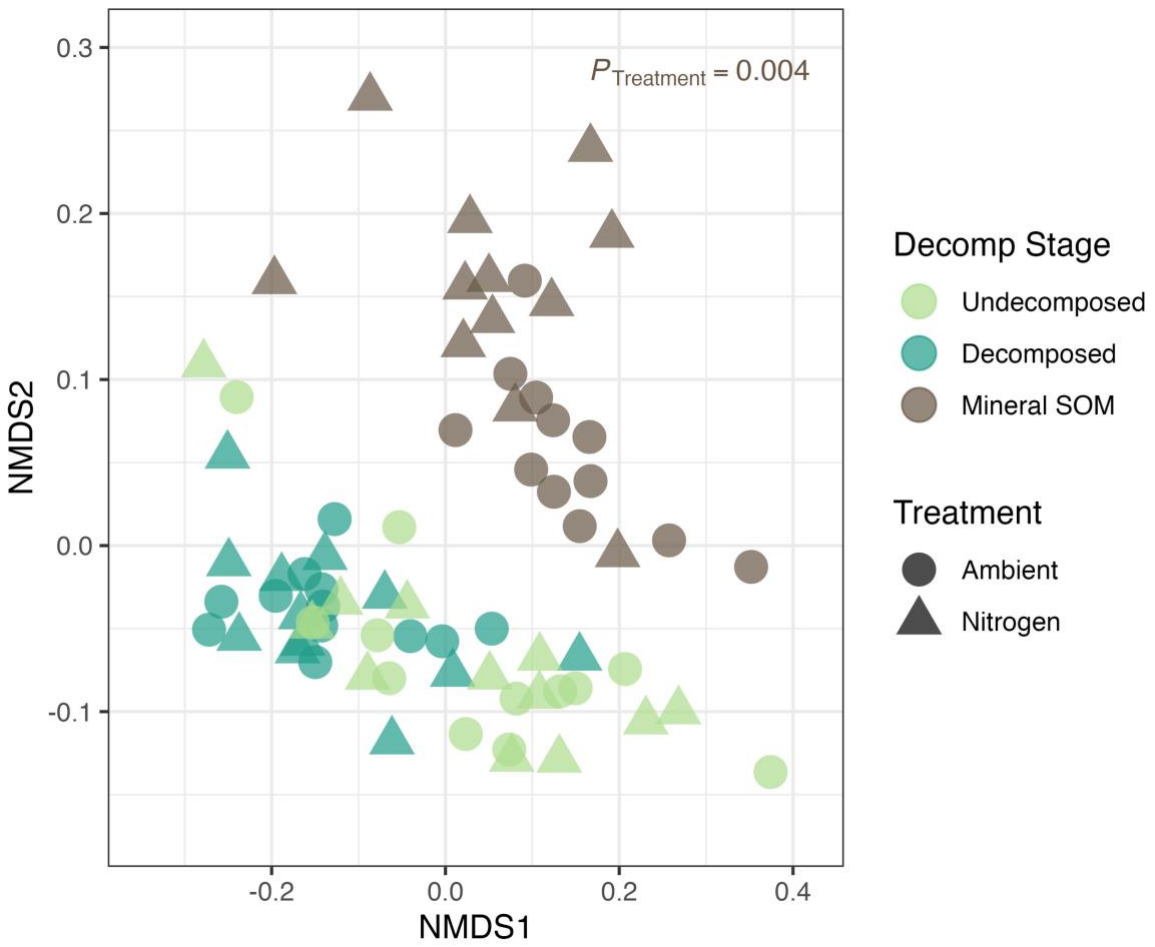

Figure 2. First two axes of non-metric multidimensional scaling (NMDS) ordination of Euclidean distances of $\log_2$ transformed py-GC/MS biochemical composition of individual samples (n = 72, k = 3, stress = 0.10). Data points represent the biochemical profile of each sample (n = 6 samples per site) and are colored by decomposition stage. The shape of the point represents if it received the ambient or the 30 kg NO_3^-–N ha^{-1} yr^{-1} nitrogen deposition treatment.

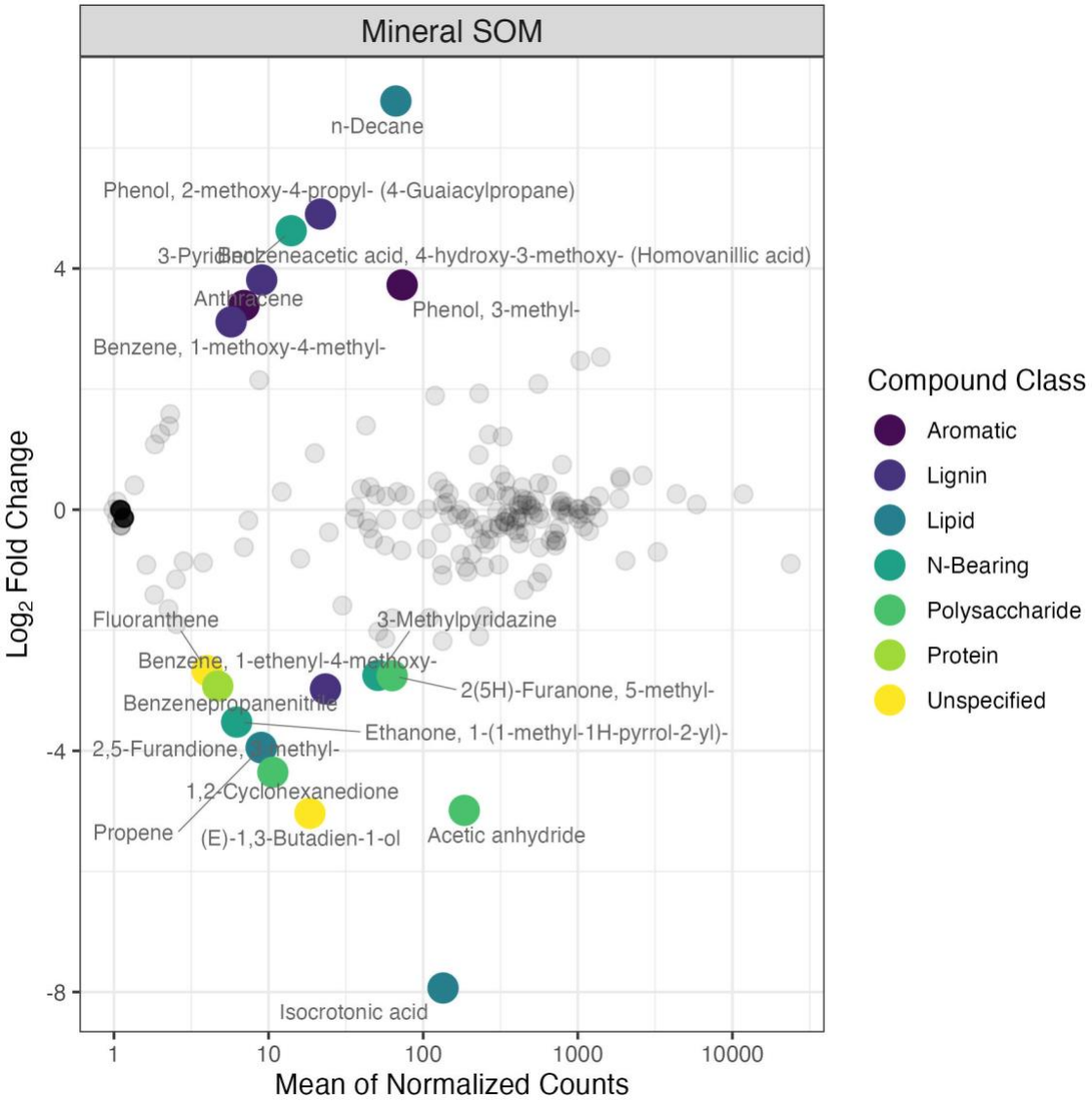

Figure 3. MA plot of the Log_2 Fold Change over the Mean of Normalized Counts for the mineral SOM py-GC/MS compounds comparing compound abundance between the ambient and nitrogen deposition treatments. Compounds with a $P_{adj} < 0.1$ are colored by their compound source class. Colored compounds above the 0 line indicate significantly higher abundance in the nitrogen deposition treatment, as compared to the ambient treatment, and vice versa for below the 0 line. For significant compound test statistics, see Table S7.

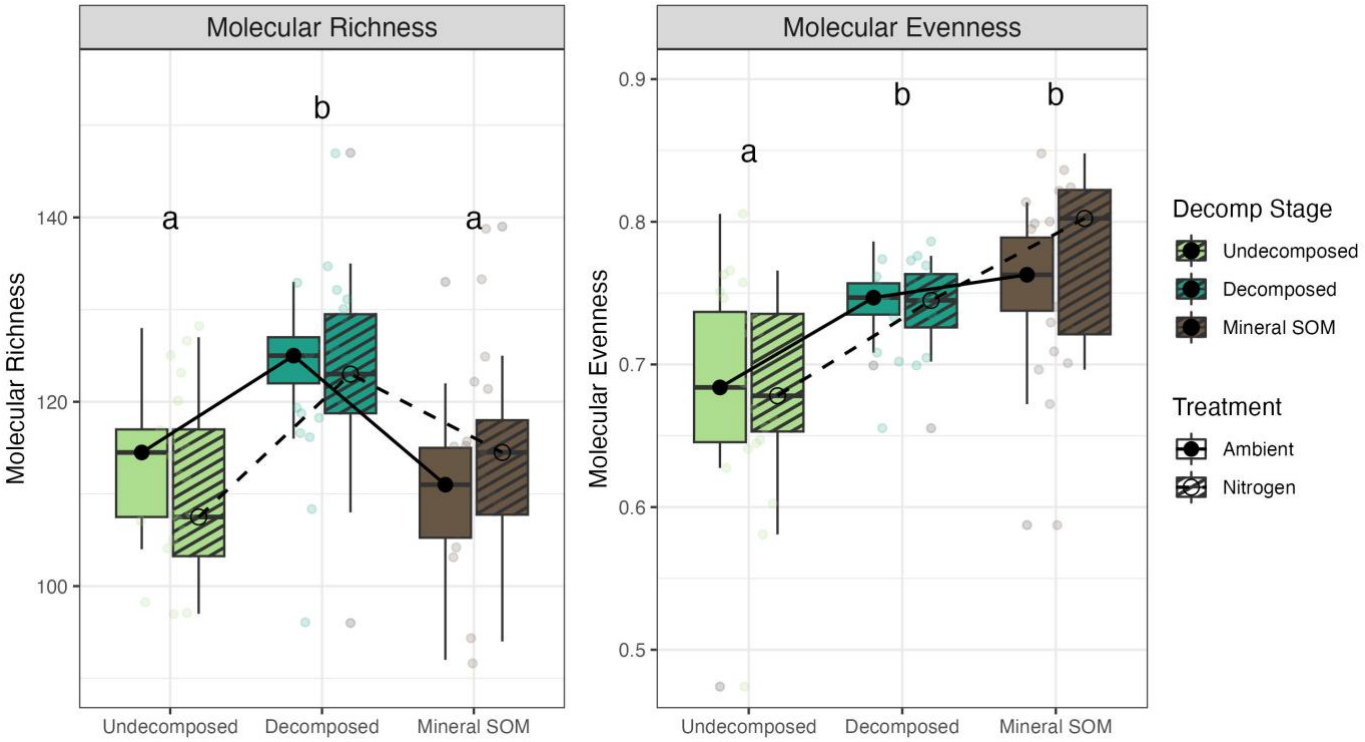

Figure 4. The effect of the nitrogen deposition treatment and decomposition stage on molecular richness (left) and evenness (right). Within each figure, ambient values are displayed on the left (solid) and nitrogen deposition treatment values are displayed on the right (dashed) for each decomposition stage (n = 3). Individual sample values (n = 72) are displayed. Two-way ANOVA was used to test the effect of Decomposition Stage, Treatment, and Decomposition Stage x Treatment interaction. The effect of Decomposition Stage was significant for both richness (F_{decomp} = 9.49, P <0.001) and evenness (F_{decomp} = 12.22, P<0.001). Decomposition Stage pairwise comparisons (Tukey's HSD) are displayed as letters (see Supplementary Table S9).

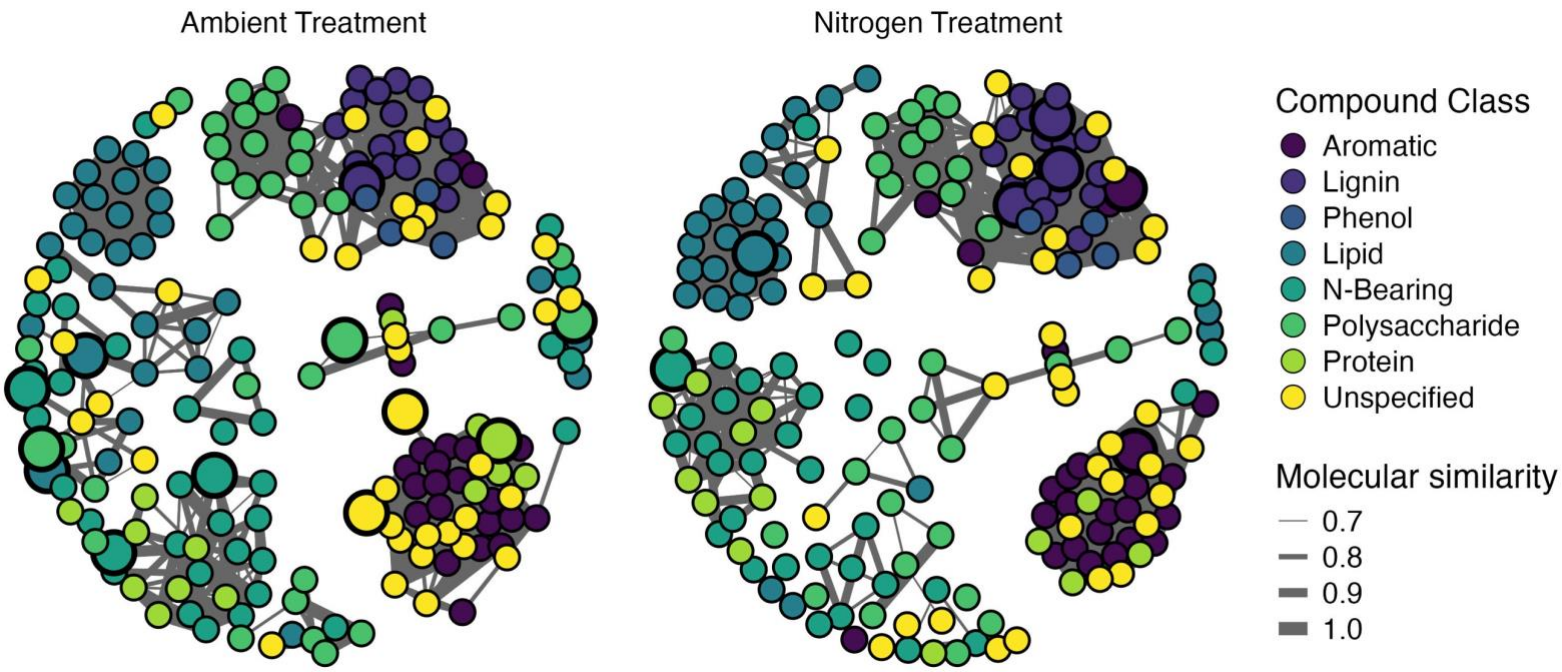

Figure 5. Molecular network showing relationships between the biochemical compounds present in the mineral SOM under ambient (left) and nitrogen deposition (right) conditions. Nodes represent individual molecules (ambient: n = 197; nitrogen treatment: n = 189) and edges represent the quantity of interactions and relationships between those molecules (ambient: n = 2450; nitrogen treatment: n = 2502). Thickness of the edges is determined by the molecular similarity of which the cut off value was set to 0.7. Nodes are colored by the compound class to which that individual molecule belongs. Enlarged nodes represent the molecules in greater abundance in that treatment from differential abundance analysis (Fig. 4).

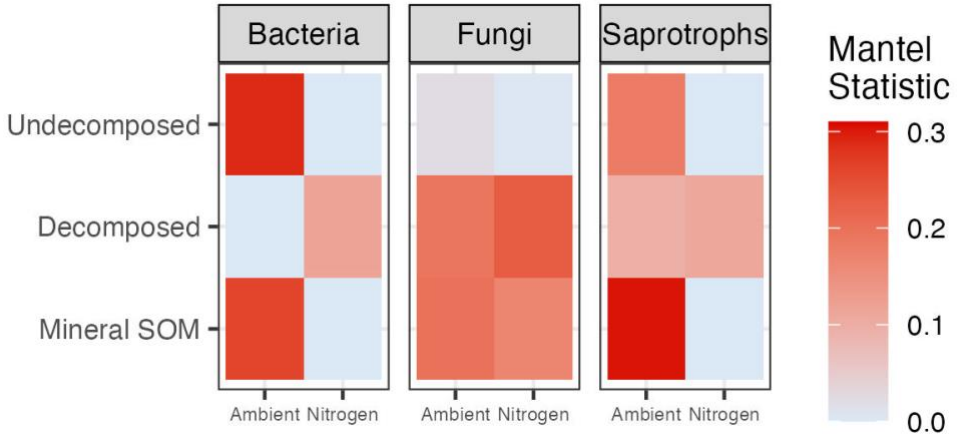

Figure 6. Mantel statistic (R) for the relationships between the bacterial (left), fungal (middle), and saprotrophic (right) communities and the biochemistry of the organic matter at each decomposition stage. Higher R values indicate stronger relationships (red). See Table S10 for full Mantel statistics.

Table S1. Site, climate, vegetation, and soil characteristics of the four northern hardwood forest stands in Michigan, USA (see Figure 2). The sites exist across a natural north-south climatic gradient, yet are similar in age, plant composition, and soil development.

Characteristic	Site A	Site B	Site C	Site D
Location				
Latitude (N)	46°52’	45°*33*’	44°*23*’	43°*40*’
Longitude (W)	*88*°53’	*84*°52’	*85*°50’	*86°09*’
Climate				
Mean annual temperature (°*C*)	4.7	6.0	6.9	7.6
Mean annual precipitation (m*m*)	873	871	888	812
Ambient wet + dry total N deposition ($g\ m^{-2}\ yr^{-1}$)	0.68	0.91	1.17	1.18
Growing season length (days)	134	150	154	157
Vegetation				
Overstory biomass ($Mg\ ha^{-1}$)	261	261	274	234
Acer saccharum biomass ($Mg\ ha^{-1}$)	237	224	216	201
Soil				
Soil texture (0-10cm) (%sand-%silt-%clay)	75:22:3	89:9:2	89:9:2	87:10:3

875 **Table S2.** Two-way ANOVA results for the effect of Site, Treatment, and Site x Treatment

876 interaction on $\log_2$-transformed relative abundances of the 8 compounds classes in Mineral Soil

877 Organic Matter (SOM). Significant P-values ($P \leq 0.1$) are presented in bold.

Compound class	Factor	Numerator df	Denominator df	F-value	P-value
Aromatic	Site	3	20	2.5041	**0.0962**
	Treatment	1	22	1.4847	0.2407
	Site x Treatment	3	20	0.5880	0.6316
Lignin	Site	3	20	6.3903	**0.0047**
	Treatment	1	22	3.2040	**0.0924**
	Site x Treatment	3	20	0.4467	0.7230
Lipid	Site	3	20	1.2469	0.3257
	Treatment	1	22	1.5861	0.2259
	Site x Treatment	3	20	0.1884	0.9027
N-Bearing	Site	3	20	7.3233	**0.0026**
	Treatment	1	22	0.8199	0.3786
	Site x Treatment	3	20	2.9805	**0.0626**
Phenol	Site	3	20	0.6791	0.5775
	Treatment	1	22	2.9435	0.1055
	Site x Treatment	3	20	0.4292	0.7349
Polysaccharide	Site	3	20	0.5502	0.6552
	Treatment	1	22	0.4042	0.5339
	Site x Treatment	3	20	4.5208	**0.0177**
Protein	Site	3	20	1.7234	0.2024
	Treatment	1	22	0.5559	0.4667
	Site x Treatment	3	20	0.3023	0.8233
Unspecified	Site	3	20	1.1552	0.3574
	Treatment	1	22	0.4160	0.5281
	Site x Treatment	3	20	0.8866	0.4691

878

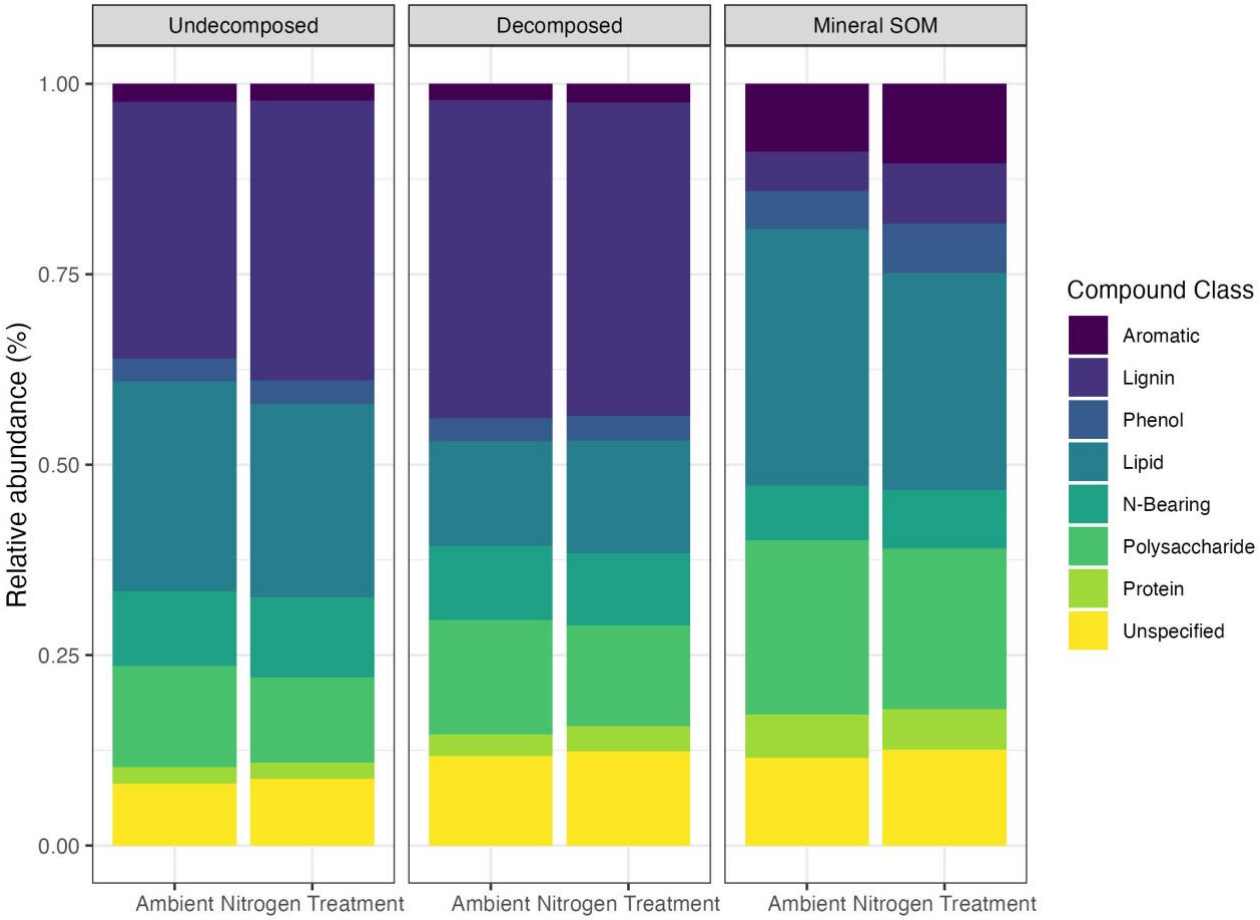

Figure S1. Stacked abundance chart of the relative abundances of the 8 compound classes across the three decomposition stages from least (left, Undecomposed) to most (right, Mineral SOM) decomposed under ambient and simulated nitrogen deposition conditions. Across the three decomposition stages, the nitrogen deposition treatment only significantly affected the relative abundance of lignin in the mineral SOM (+53% in nitrogen treatment, $P = 0.09$).

885 **Table S3.** Two-way ANOVA results for the effect of Site, Treatment, and Site x Treatment

886 interaction on log_2-transformed relative abundances of the 8 compounds classes in

887 Undecomposed fine roots. Significant P-values ($P \leq 0.1$) are presented in bold.

Compound class	Factor	Numerator df	Denominator df	F-value	P-value
Aromatic	Site	3	20	0.9337	0.4473
	Treatment	1	22	0.2609	0.6165
	Site x Treatment	3	20	2.1511	0.1338
Lignin	Site	3	20	0.0870	0.9662
	Treatment	1	22	0.4924	0.4929
	Site x Treatment	3	20	1.2213	0.3343
Lipid	Site	3	20	1.1512	0.3588
	Treatment	1	22	0.1842	0.6735
	Site x Treatment	3	20	1.1179	0.3711
N-Bearing	Site	3	20	2.7075	**0.0799**
	Treatment	1	22	0.4525	0.5108
	Site x Treatment	3	20	1.1713	0.3516
Phenol	Site	3	20	1.5606	0.2378
	Treatment	1	22	0.3278	0.5749
	Site x Treatment	3	20	4.5536	**0.0173**
Polysaccharide	Site	3	20	4.3391	**0.0203**
	Treatment	1	22	1.5337	0.2334
	Site x Treatment	3	20	3.9589	**0.0275**
Protein	Site	3	20	0.7584	0.5337
	Treatment	1	22	0.0003	0.9860
	Site x Treatment	3	20	0.5795	0.6369
Unspecified	Site	3	20	1.5001	0.2526
	Treatment	1	22	0.3898	0.5412
	Site x Treatment	3	20	1.3106	0.3054

888

Table S4. Two-way ANOVA results for the effect of Site, Treatment, and Site x Treatment interaction on $\log_2$-transformed relative abundances of the 8 compounds classes in the 1-yr Decomposed fine roots. Significant P-values ($P \leq 0.1$) are presented in bold.

Compound class	Factor	Numerator df	Denominator df	F-value	P-value
Aromatic	Site	3	20	3.5241	**0.0393**
	Treatment	1	22	0.7394	0.4026
	Site x Treatment	3	20	1.4160	0.2747
Lignin	Site	3	20	0.3242	0.8078
	Treatment	1	22	0.0587	0.8116
	Site x Treatment	3	20	1.4453	0.2668
Lipid	Site	3	20	1.1059	0.3757
	Treatment	1	22	0.0909	0.7669
	Site x Treatment	3	20	1.5248	0.2464
N-Bearing	Site	3	20	2.2232	0.1250
	Treatment	1	22	0.1254	0.7279
	Site x Treatment	3	20	0.2880	0.8334
Phenol	Site	3	20	2.2061	0.1270
	Treatment	1	22	0.4187	0.5267
	Site x Treatment	3	20	0.6662	0.5849
Polysaccharide	Site	3	20	2.5255	**0.0943**
	Treatment	1	22	1.3879	0.2560
	Site x Treatment	3	20	0.5719	0.6416
Protein	Site	3	20	2.4745	**0.0988**
	Treatment	1	22	2.6923	0.1203
	Site x Treatment	3	20	4.2287	**0.0222**
Unspecified	Site	3	20	0.1201	0.9469
	Treatment	1	22	0.3110	0.5848
	Site x Treatment	3	20	0.2234	0.8787

Table S5. Three-way PERMANOVA results for the effect of Decomposition Stage, Site, Treatment, and their interactions on $\log_2$-transformed Euclidean distance matrices of individual compound abundances. Below the three-way PERMANOVA results are pairwise two-way PERMANOVA results for the effect of Site, Treatment, and their interaction at the three decomposition stages. Significant P-values ($P \leq 0.1$) are presented in bold.

Decomp Stage	Factor	Df	R^2	F-value	P-value
	Decomp Stage	2	0.35930	20.707	**0.001**
	Site	3	0.01930	0.7416	0.645
	Treatment	1	0.01351	1.5572	0.193
	Decomp Stage x Site	6	0.06012	1.1548	0.312
	Decomp Stage x Treatment	2	0.02397	1.3816	0.211
	Site x Treatment	3	0.01440	0.5531	0.843
	Decomp Stage x Site x Treatment	6	0.09296	1.7858	**0.048**
Undecomposed	Site	3	0.12377	0.9610	0.444
	Treatment	1	0.00765	0.1783	0.934
	Site x Treatment	3	0.17265	1.4107	0.212
Decomposed	Site	3	0.13225	1.0294	0.405
	Treatment	1	0.00869	0.2028	0.924
	Site x Treatment	3	0.17384	1.3530	0.244
Mineral SOM	Site	3	0.11883	1.0912	0.362
	Treatment	1	0.15467	4.2612	**0.004**
	Site x Treatment	3	0.14573	1.3382	0.197

Table S6. Permutation test for homogeneity of multivariate dispersion results for the effect of Treatment on log_2-transformed Euclidean distance matrices of individual compound abundances at each of the three decomposition stages.

Decomp Stage	Factor	Df	F-value	P-value
Undecomposed	Treatment	1	0.0949	0.756
Decomposed	Treatment	1	0.2859	0.612
Mineral SOM	Treatment	1	1.7029	0.213

Table S7. Mineral SOM compounds with significant differential abundance (Benjamini-Hochberg $P_{adj} \leq 0.1$) and Log_2 fold change values that are plotted in Figure 4. Treatment refers to the treatment that the compound exhibits significantly greater abundance in.

Compound	Compound Class	Treatment	Log_2 Fold Change	Standard Error	Wald Statistic	BH P_{adj}
Phenol, 3-methyl-	Aromatic	Nitrogen	3.72780	1.12256	3.32081	0.01017
Anthracene	Aromatic	Nitrogen	3.38703	0.94245	3.59388	0.00462
Phenol, 2-methoxy-4-propyl- (4-Guaiacylpropane)	Lignin	Nitrogen	4.90243	0.97139	5.04680	0.00003
Benzeneacetic acid, 4-hydroxy-3-methoxy- (Homovanillic acid)	Lignin	Nitrogen	3.81029	0.94943	4.01324	0.00127
Benzene, 1-methoxy-4-methyl-	Lignin	Nitrogen	3.11383	0.90764	3.43070	0.00787
Benzene, 1-ethenyl-4-methoxy-	Lignin	Ambient	-2.97359	1.01665	-2.92489	0.03446
n-Decane	Lipid	Nitrogen	6.77821	1.05588	6.41951	<0.0001
Propene	Lipid	Ambient	-3.95030	1.01705	-3.88408	0.00183
Isocrotonic acid	Lipid	Ambient	-7.93390	1.07392	-7.38778	<0.0001
3-Pyridinol	N-Bearing	Nitrogen	4.62658	1.06348	4.35040	0.00039
3-Methylpyridazine	N-Bearing	Ambient	-2.74810	1.00508	-2.73422	0.05905
Ethanone, 1-(1-methyl-1H-pyrrol-2-yl)-	N-Bearing	Ambient	-3.52273	0.92806	-3.79581	0.00227
2,5-Furandione, 3-methyl-	N-Bearing	Ambient	-3.94198	1.01805	-3.87210	0.00183
2(5H)-Furanone, 5-methyl-	Polysaccharide	Ambient	-2.75395	1.07045	-2.57270	0.09029
1,2-Cyclohexanedione	Polysaccharide	Ambient	-4.35563	1.04552	-4.16602	0.00075
Acetic anhydride	Polysaccharide	Ambient	-4.98762	1.09738	-4.54501	0.00019
Benzenepropanenitrile	Protein	Ambient	-2.92576	0.86588	-3.37895	0.00884
Fluoranthene	Unspecified	Ambient	-2.66957	0.83642	-3.19167	0.01503
(E)-1,3-Butadien-1-ol	Unspecified	Ambient	-5.03650	1.09046	-4.61868	0.00016

Table S8. Two-way ANOVA results for the effect of Decomposition Stage, Treatment, and Decomposition Stage x Treatment interaction on molecular richness (top) and molecular evenness (bottom) diversity metrics. Significant P-values ($P \leq 0.1$) are presented in bold.

Diversity Metric	Factor	Numerator df	Denominator df	F-value	P-value
Molecular Richness	Decomp Stage	2	69	9.4898	**<0.001**
	Treatment	1	70	0.0016	0.9686
	Decomp Stage x Treatment	2	69	0.3979	0.6733
Molecular Evenness	Decomp Stage	2	69	12.224	**<0.001**
	Treatment	1	70	0.3925	0.5331
	Decomp Stage x Treatment	2	69	0.6333	0.5340

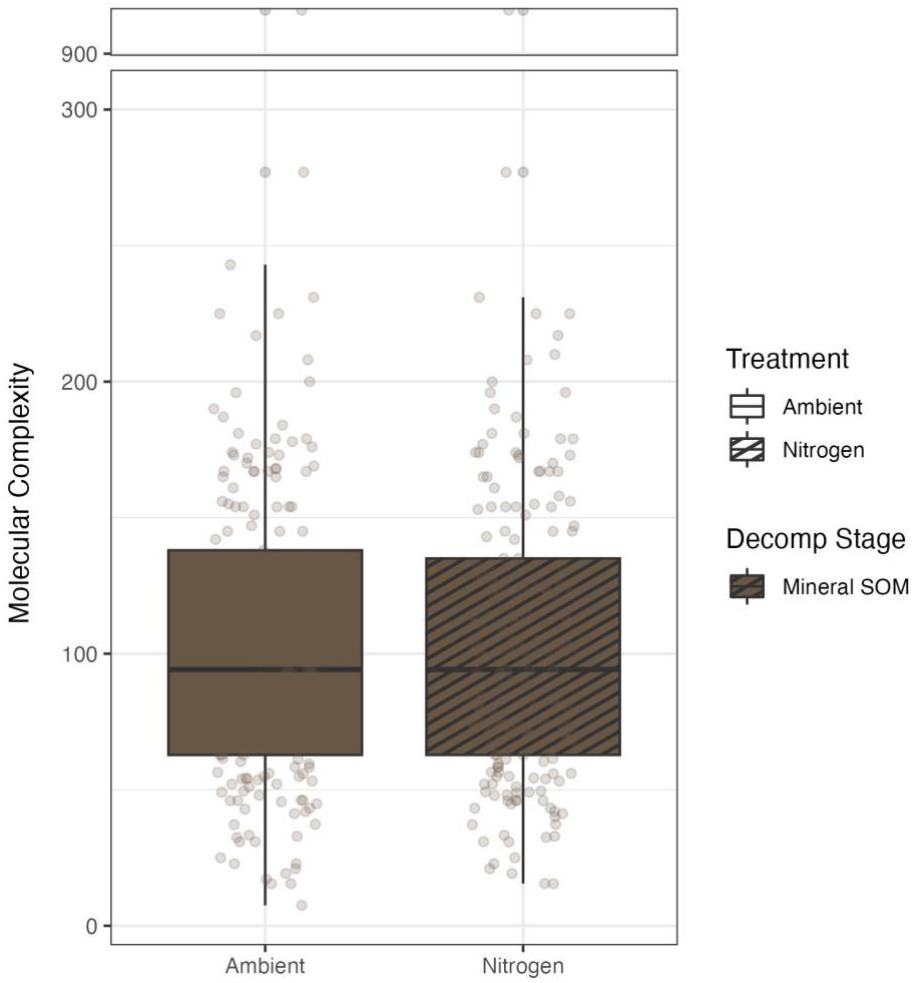

Figure S2. The effect of the nitrogen deposition treatment on the molecular complexity of individual biochemical compounds present in the Mineral SOM (n = 386). No treatment effect was detected by ANOVA ($F_{1,384} = 0$, $P = 0.997$).

Table S9. Tukey's HSD pairwise comparisons where two-way ANOVA of molecular diversity metrics revealed significant ($P \leq 0.1$) effect of Decomposition Stage on molecular richness (top) and evenness (bottom) (see Supplementary Table S8). Significant P-values ($P \leq 0.1$) are presented in bold.

Diversity Metric	Factor	Post-hoc Comparison	Mean Difference	P-value
Molecular Richness	Decomp Stage	Undecomposed – Decomposed	-12.8750	**0.0011**
		Decomposed – Mineral SOM	13.0833	**<0.001**
		Undecomposed – Mineral SOM	0.2083	0.9980
	Decomp Stage x Treatment	Ambient Undecomposed – Ambient Decomposed	-12.5833	**0.0316**
		Ambient Decomposed – Ambient Mineral SOM	3.0000	0.8116
		Ambient Undecomposed – Ambient Mineral SOM	15.5833	**0.0059**
		Nitrogen Undecomposed – Nitrogen Decomposed	-13.1667	**0.0232**
		Nitrogen Decomposed – Nitrogen Mineral SOM	10.5834	**0.0830**
		Nitrogen Undecomposed – Nitrogen Mineral SOM	-2.5833	0.8565
Molecular Evenness	Decomp Stage	Undecomposed – Decomposed	-0.0580	**0.0026**
		Decomposed – Mineral SOM	-0.0220	0.3902
		Undecomposed – Mineral SOM	-0.0800	**<0.001**
	Decomp Stage x Treatment	Ambient Undecomposed – Ambient Decomposed	-0.0624	**0.0274**
		Ambient Decomposed – Ambient Mineral SOM	-0.0040	0.9843
		Ambient Undecomposed – Ambient Mineral SOM	-0.0664	**0.0176**
		Nitrogen Undecomposed – Nitrogen Decomposed	-0.0536	**0.0673**
		Nitrogen Decomposed – Nitrogen Mineral SOM	-0.0401	0.2136
		Nitrogen Undecomposed – Nitrogen Mineral SOM	-0.0937	**0.0005**

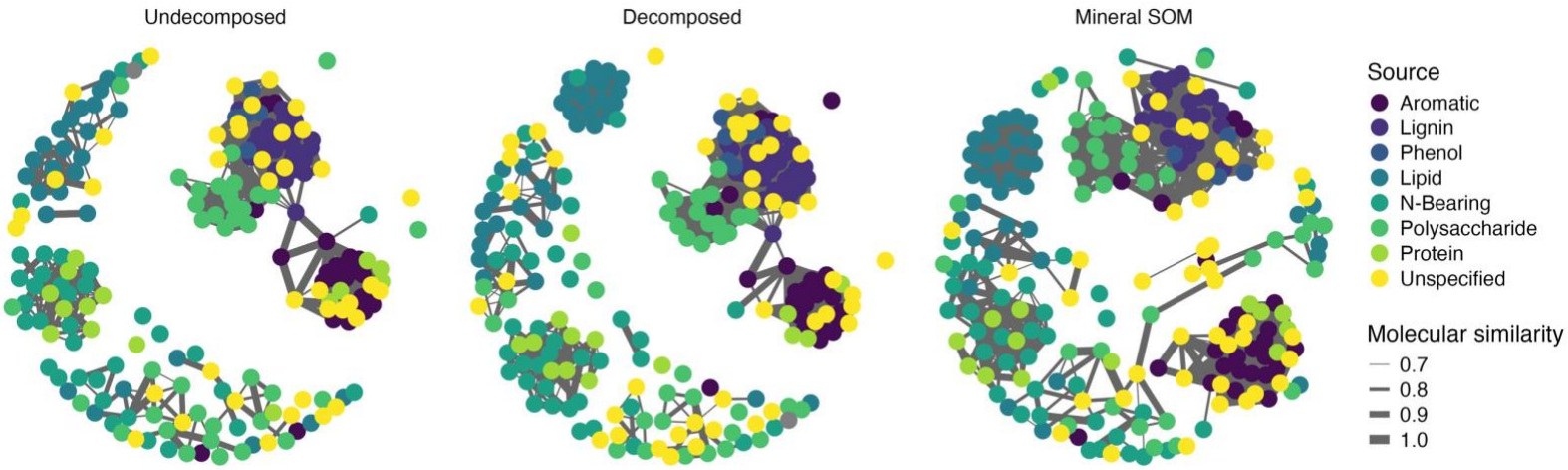

Figure S3. Molecular network showing relationships between the biochemical compounds at each decomposition stage (n = 3). Nodes represent individual molecules (Undecomposed: n = 209; Decomposed: n = 225, Mineral SOM: n = 216) and edges represent the quantity of interactions and relationships between those molecules (Undecomposed: n = 2950; Decomposed: n = 3372, Mineral SOM: n = 3020). Thickness of the edges is determined by the molecular similarity of which the cut off value was set to 0.7. Nodes are colored by their relative abundance.

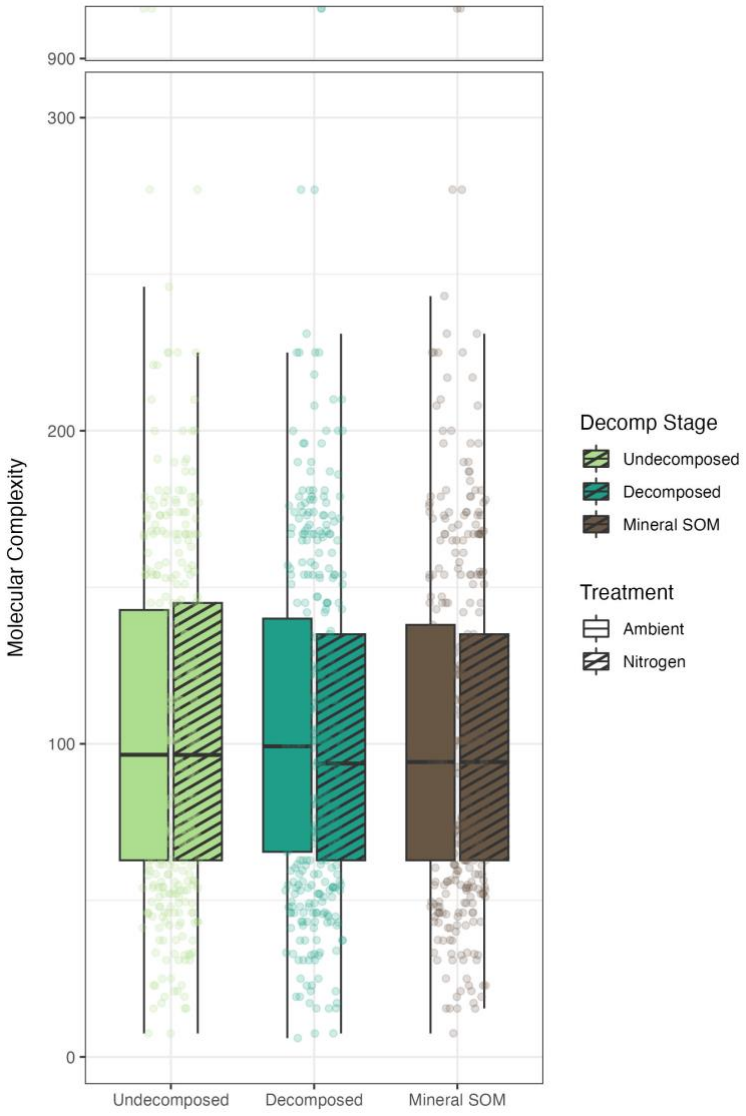

Figure S4. The effect of decomposition and the nitrogen deposition treatment on the molecular complexity of individual biochemical compounds present at each decomposition stage (n_{total} = 1182). ANOVA detected no difference in decomposition stage (F = 0.01, P = 0.989), treatment (F = 0.03, P = 0.852), or their interaction (F = 0.02, P = 0.976).

964 **Table S10.** Mantel test results comparing $\log_2$-transformed Euclidean distance matrices of

965 individual compound abundances and Hellinger-transformed Bray-Curtis distance matrices of

966 microbial community OTU abundances. Significant P-values ($P \leq 0.1$) are presented in bold.

Type	Treatment	Decomp Stage	Mantel Statistic (R)	P-value	Upper quantiles of permutations (null model) 90%	95%	97.5%	99%
Bacteria (16S)	Ambient	Undecomposed	**0.288700**	**0.069**	0.255	0.314	0.360	0.406
		Decomposed	-0.001153	0.476	0.245	0.339	0.428	0.474
		Mineral SOM	0.2607	0.123	0.296	0.375	0.426	0.467
	Nitrogen	Undecomposed	-0.2065	0.912	0.227	0.278	0.328	0.371
		Decomposed	0.117	0.211	0.278	0.376	0.441	0.518
		Mineral SOM	-0.1325	0.720	0.261	0.321	0.384	0.425
Fungi (28S)	Ambient	Undecomposed	0.02193	0.455	0.203	0.251	0.299	0.341
		Decomposed	0.1921	0.107	0.200	0.237	0.273	0.326
		Mineral SOM	**0.1981**	**0.091**	0.187	0.239	0.292	0.328
	Nitrogen	Undecomposed	0.002091	0.473	0.161	0.210	0.243	0.290
		Decomposed	**0.2292**	**0.041**	0.175	0.208	0.246	0.298
		Mineral SOM	0.1662	0.105	0.170	0.216	0.243	0.298
Saprotrophs	Ambient	Undecomposed	0.1829	0.148	0.230	0.275	0.316	0.359
		Decomposed	0.09608	0.290	0.229	0.284	0.363	0.413
		Mineral SOM	**0.3031**	**0.064**	0.240	0.319	0.368	0.411
	Nitrogen	Undecomposed	-0.01454	0.518	0.229	0.281	0.335	0.382
		Decomposed	0.1114	0.242	0.256	0.336	0.408	0.467
		Mineral SOM	-0.1032	0.681	0.281	0.347	0.382	0.449

967

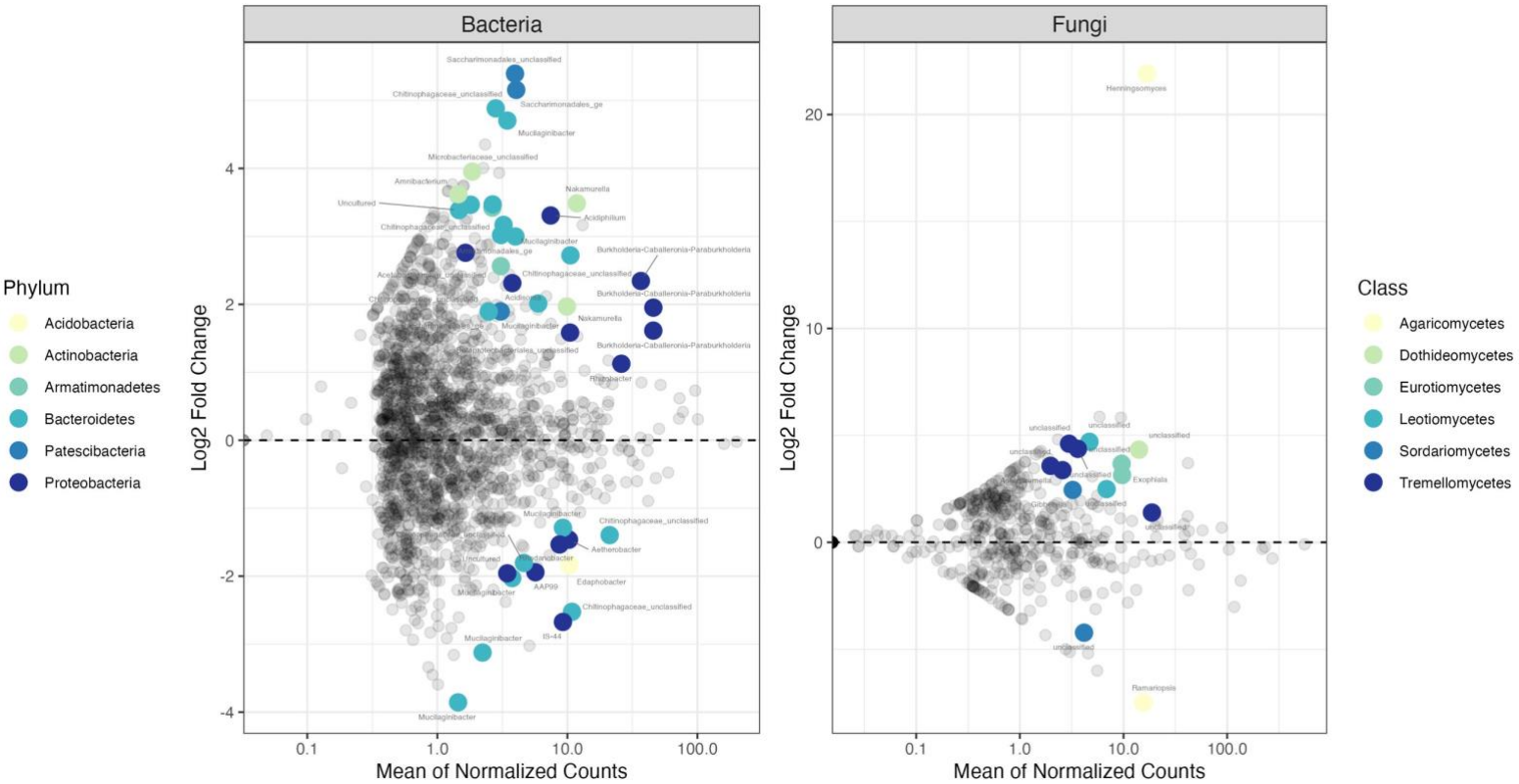

Figure S4. Plot of the Log_2 Fold Change over the Mean of Normalized Counts for the bacteria (left) and fungi (right) genera comparing species abundance between the ambient and nitrogen deposition treatments in the "decomposed" samples. Species with a $p_{adj} < 0.1$ are colored by phylum. Colored species above the 0 line indicate a significantly higher abundance in the nitrogen deposition treatment, as compared to the ambient treatment, and vice versa for below the 0 line.

Table S11. Bacteria with significant differential abundance (Benjamini-Hochberg $P_{adj} \leq 0.1$) and Log_2 fold change values that are plotted in Figure S4 (left). Treatment refers to the treatment that the OTU (species) exhibits significantly greater abundance in.

Kingdom	Phylum	Class	Order	Family	Genus	Treatment	Log_2 Fold Change	Standard Error	Wald Statistic	BH P_{adj}
Bacteria	Patescibacteria	Saccharimonadia	Saccharimonadales	Unclassified	Unclassified	Nitrogen	5.39412	1.50297	3.58898	0.01505
Bacteria	Patescibacteria	Saccharimonadia	Saccharimonadales	Unclassified	Unclassified	Nitrogen	5.15561	1.19097	4.32891	0.00322
Bacteria	Bacteroidetes	Bacteroidia	Chitinophagales	Chitinophagaceae	Unclassified	Nitrogen	4.88380	1.29715	3.76504	0.01029
Bacteria	Bacteroidetes	Bacteroidia	Sphingobacteriales	Sphingobacteriaceae	Mucilaginibacter	Nitrogen	4.70389	0.84858	5.54322	0.00001
Bacteria	Actinobacteria	Actinobacteria	Micrococcales	Microbacteriaceae	Unclassified	Nitrogen	3.95287	1.29021	3.06375	0.05308
Bacteria	Actinobacteria	Actinobacteria	Micrococcales	Microbacteriaceae	Amnibacterium	Nitrogen	3.62117	1.18129	3.06544	0.05308
Bacteria	Actinobacteria	Actinobacteria	Frankiales	Nakamurellaceae	Nakamurella	Nitrogen	3.48676	1.03957	3.35404	0.02843
Bacteria	Bacteroidetes	Bacteroidia	Chitinophagales	Chitinophagaceae	Ferruginibacter	Nitrogen	3.47086	1.25134	2.77371	0.09754
Bacteria	Bacteroidetes	Bacteroidia	Chitinophagales	Chitinophagaceae	Unclassified	Nitrogen	3.46616	1.15698	2.99588	0.06041
Bacteria	Armatimonadetes	Armatimonadia	Armatimonadales	Unclassified	Unclassified	Nitrogen	3.42300	0.93394	3.66513	0.01401
Bacteria	Bacteroidetes	Bacteroidia	Chitinophagales	Chitinophagaceae	Uncultured	Nitrogen	3.38620	0.95645	3.54038	0.01688
Bacteria	Proteobacteria	Alphaproteobacteria	Acetobacterales	Acetobacteraceae	Acidiphilium	Nitrogen	3.30733	0.93798	3.52600	0.01688
Bacteria	Bacteroidetes	Bacteroidia	Chitinophagales	Chitinophagaceae	Unclassified	Nitrogen	3.16901	1.14426	2.76950	0.09754
Bacteria	Bacteroidetes	Bacteroidia	Chitinophagales	Chitinophagaceae	Unclassified	Nitrogen	3.02005	1.05278	2.86863	0.08495
Bacteria	Bacteroidetes	Bacteroidia	Sphingobacteriales	Sphingobacteriaceae	Mucilaginibacter	Nitrogen	2.99831	1.07783	2.78179	0.09754
Bacteria	Proteobacteria	Alphaproteobacteria	Acetobacterales	Acetobacteraceae	Unclassified	Nitrogen	2.75872	0.95259	2.89603	0.08031
Bacteria	Bacteroidetes	Bacteroidia	Chitinophagales	Chitinophagaceae	Unclassified	Nitrogen	2.72105	0.90886	2.99392	0.06041
Bacteria	Armatimonadetes	Armatimonadia	Armatimonadales	Unclassified	Unclassified	Nitrogen	2.56260	0.74517	3.43895	0.02206
Bacteria	Proteobacteria	Gammaproteobacteria	Betaproteobacteriales	Burkholderiaceae	Burkholderia-Caballeronia-Paraburkholderia	Nitrogen	2.34356	0.62196	3.76802	0.01029
Bacteria	Proteobacteria	Alphaproteobacteria	Acetobacterales	Acetobacteraceae	Acidisoma	Nitrogen	2.31260	0.59484	3.88776	0.00860
Bacteria	Bacteroidetes	Bacteroidia	Chitinophagales	Chitinophagaceae	Uncultured	Nitrogen	3.38620	0.95645	3.54038	0.01688
Bacteria	Proteobacteria	Alphaproteobacteria	Acetobacterales	Acetobacteraceae	Acidiphilium	Nitrogen	3.30733	0.93798	3.52600	0.01688
Bacteria	Bacteroidetes	Bacteroidia	Sphingobacteriales	Sphingobacteriaceae	Mucilaginibacter	Nitrogen	2.01288	0.51097	3.93931	0.00794
Bacteria	Actinobacteria	Actinobacteria	Frankiales	Nakamurellaceae	Nakamurella	Nitrogen	1.96852	0.60164	3.27192	0.03310
Bacteria	Proteobacteria	Gammaproteobacteria	Betaproteobacteriales	Burkholderiaceae	Burkholderia-Caballeronia-Paraburkholderia	Nitrogen	1.95134	0.62661	3.11412	0.04825

Bacteria	Patescibacteria	Saccharimonadia	Saccharimonadales	Unclassified	Unclassified	Nitrogen	1.89504	0.68840	2.75283	0.09799
Bacteria	Bacteroidetes	Bacteroidia	Chitinophagales	Chitinophagaceae	Unclassified	Nitrogen	1.89319	0.67628	2.79941	0.09754
Bacteria	Proteobacteria	Gammaproteobacteria	Betaproteobacteriales	Burkholderiaceae	Burkholderia-Caballeronia-Paraburkholderia	Nitrogen	1.61355	0.44282	3.64382	0.01405
Bacteria	Proteobacteria	Gammaproteobacteria	Betaproteobacteriales	Unclassified	Unclassified	Nitrogen	1.58444	0.48965	3.23585	0.03436
Bacteria	Proteobacteria	Gammaproteobacteria	Betaproteobacteriales	Burkholderiaceae	Rhizobacter	Nitrogen	1.12582	0.29837	3.77320	0.01029
Bacteria	Bacteroidetes	Bacteroidia	Sphingobacteriales	Sphingobacteriaceae	Mucilaginibacter	Ambient	-1.28789	0.40941	-3.14574	0.04506
Bacteria	Bacteroidetes	Bacteroidia	Chitinophagales	Chitinophagaceae	Unclassified	Ambient	-1.39623	0.42964	-3.24976	0.03415
Bacteria	Proteobacteria	Deltaproteobacteria	Myxococcales	Polyangiaceae	Aetherobacter	Ambient	-1.46319	0.40563	-3.60718	0.01504
Bacteria	Proteobacteria	Gammaproteobacteria	Xanthomonadales	Rhodanobacteraceae	Rhodanobacter	Ambient	-1.53376	0.38863	-3.94662	0.00794
Bacteria	Bacteroidetes	Bacteroidia	Chitinophagales	Chitinophagaceae	Unclassified	Ambient	-1.80558	0.45541	-3.96475	0.00794
Bacteria	Acidobacteria	Acidobacteriia	Acidobacteriales	Acidobacteriaceae_	Edaphobacter	Ambient	-1.83235	0.64683	-2.83280	0.09228
Bacteria	Proteobacteria	Gammaproteobacteria	Betaproteobacteriales	Burkholderiaceae	AAP99	Ambient	-1.94233	0.45411	-4.27721	0.00322
Bacteria	Proteobacteria	Alphaproteobacteria	Micropepsales	Micropepsaceae	Uncultured	Ambient	-1.95804	0.65177	-3.00419	0.06041
Bacteria	Bacteroidetes	Bacteroidia	Sphingobacteriales	Sphingobacteriaceae	Mucilaginibacter	Ambient	-2.02805	0.60709	-3.34058	0.02843
Bacteria	Bacteroidetes	Bacteroidia	Chitinophagales	Chitinophagaceae	Unclassified	Ambient	-2.52434	0.44489	-5.67414	0.00001
Bacteria	Proteobacteria	Gammaproteobacteria	Betaproteobacteriales	Nitrosomonadaceae	IS-44	Ambient	-2.67385	0.95610	-2.79662	0.09754
Bacteria	Bacteroidetes	Bacteroidia	Sphingobacteriales	Sphingobacteriaceae	Mucilaginibacter	Ambient	-3.12362	1.13077	-2.76239	0.09754
Bacteria	Bacteroidetes	Bacteroidia	Sphingobacteriales	Sphingobacteriaceae	Mucilaginibacter	Ambient	-3.85663	1.17895	-3.27124	0.03310

Table S12. Fungi with significant differential abundance (Benjamini-Hochberg $P_{\mathrm{adj}} \leq 0.1$) and Log_2 fold change values that are plotted in Figure S4 (right). Treatment refers to the treatment that the OTU (species) exhibits significantly greater abundance in.

Kingdom	Phylum	Class	Order	Family	Genus	Treatment	Log_2 Fold Change	Standard Error	Wald Statistic	BH P_{adj}
Fungi	Basidiomycota	Agaricomycetes	Agaricales	Schizophyllaceae	Henningsomyces	Nitrogen	21.90978	2.94575	7.43776	<0.00001
Fungi	Ascomycota	Leotiomycetes	Unclassified	Unclassified	Unclassified	Nitrogen	4.69786	1.43680	3.26967	0.03446
Fungi	Basidiomycota	Tremellomycetes	Tremellales	Unclassified	Unclassified	Nitrogen	4.60797	1.72523	2.67094	0.09310
Fungi	Basidiomycota	Tremellomycetes	Tremellales	Unclassified	Unclassified	Nitrogen	4.36903	1.65903	2.63349	0.09659
Fungi	Ascomycota	Dothideomycetes	Pleosporales	Unclassified	Unclassified	Nitrogen	4.33137	1.34815	3.21282	0.03505
Fungi	Ascomycota	Eurotiomycetes	Chaetothyriales	Herpotrichiellaceae	Unclassified	Nitrogen	3.67041	1.26887	2.89266	0.06651
Fungi	Basidiomycota	Tremellomycetes	Tremellales	Unclassified	Unclassified	Nitrogen	3.57464	1.02756	3.47875	0.02015
Fungi	Basidiomycota	Tremellomycetes	Tremellales	Tremellaceae	Asterotremella	Nitrogen	3.37403	1.20852	2.79186	0.06987
Fungi	Ascomycota	Eurotiomycetes	Chaetothyriales	Herpotrichiellaceae	Exophiala	Nitrogen	3.14462	1.09721	2.86602	0.06651
Fungi	Ascomycota	Leotiomycetes	Helotiales	Unclassified	Unclassified	Nitrogen	2.48835	0.79990	3.11083	0.04264
Fungi	Ascomycota	Sordariomycetes	Hypocreales	Nectriaceae	Gibberella	Nitrogen	2.44656	0.87541	2.79476	0.06987
Fungi	Basidiomycota	Tremellomycetes	Tremellales	Tremellaceae	Unclassified	Nitrogen	1.39111	0.38410	3.62174	0.01808
Fungi	Ascomycota	Sordariomycetes	Unclassified	Unclassified	Unclassified	Ambient	-4.22650	1.47236	-2.87056	0.06651
Fungi	Basidiomycota	Agaricomycetes	Agaricales	Clavariaceae	Ramariopsis	Ambient	-7.48238	2.08804	-3.58345	0.01808

982 Supplemental References:

983

984 S Xu, M Chen, T Feng, L Zhan, L Zhou, G Yu. Use ggbreak to effectively utilize plotting space

985 to deal with large datasets and outliers. Frontiers in Genetics. 2021, 12:774846.

986 https://doi:10.3389/fgene.2021.774846